# E–N-cadherin heterodimers define novel adherens junctions connecting endoderm-derived cells

Beate K. Straub,[1,2] Steffen Rickelt,[1,5] Ralf Zimbelmann,[1] Christine Grund,[1] Caecilia Kuhn,[1,5] Marcus Iken,[3,4] Michael Ott,[3,4] Peter Schirmacher,[2] and Werner W. Franke[1,5]

[1]Helmholtz Group for Cell Biology, German Cancer Research Center, 69120 Heidelberg, Germany
[2]Department of General Pathology, Institute of Pathology, University Clinic Heidelberg, 69120 Heidelberg, Germany
[3]Department of Gastroenterology, Hepatology and Endocrinology, and [4]Twincore Centre for Experimental and Clinical Infection Research, Hannover Medical School, 30625 Hannover, Germany
[5]Progen Biotechnik, 69123 Heidelberg, Germany

Intercellular junctions play a pivotal role in tissue development and function and also in tumorigenesis. In epithelial cells, decrease or loss of E-cadherin, the hallmark molecule of adherens junctions (AJs), and increase of N-cadherin are widely thought to promote carcinoma progression and metastasis. In this paper, we show that this "cadherin switch" hypothesis does not hold for diverse endoderm-derived cells and cells of tumors derived from them. We show that the cadherins in a major portion of AJs in these cells can be chemically cross-linked in E–N heterodimers. We also show that cells possessing E–N heterodimer AJs can form semistable hemihomotypic AJs with purely N-cadherin–based AJs of mesenchymally derived cells, including stroma cells. We conclude that these heterodimers are the major AJ constituents of several endoderm-derived tissues and tumors and that the prevailing concept of antagonistic roles of these two cadherins in developmental and tumor biology has to be reconsidered.

## Introduction

The ordered association of cells into tissues and their integration into functional organs is generally effected by the patterns of intercellular junctions formed by clusters of cell type–specific, cell–cell-connecting protein and glycoprotein complexes subsumed under the category of adherens junctions (AJs). Apparently, all the transmembrane glycoproteins involved belong to a large superfamily of $Ca^{2+}$-binding molecules, the cadherins, the carboxy-terminal domains of which are anchored in dense cytoplasmic plaques containing so-called *armadillo*-type and certain other proteins that can provide anchorage of intracellular cytoskeletal filaments. This architectonic system linking the functional order of the cell interior to the specific intercellular organization of the tissue is already visible in the evolutionarily first metazoa (Halbleib and Nelson, 2006) and has developed into a diversity of epithelial, mesenchymal, muscular, and neural tissues (Takeichi, 1988, 1995; Gumbiner, 2005; Franke, 2009).

Current concepts of the development of cell–cell associations are based—in the first order—on principles of homophilic cell–cell adhesion of cell type–specific, densely clustered cadherins (e.g., Hatta and Takeichi, 1986; Wheelock and Johnson, 2003; Perez and Nelson, 2004; Foty and Steinberg, 2005; Gumbiner, 2005; Shapiro and Weis, 2009). For example, epithelial cells are generally connected by the epithelial-type cadherin (E-cadherin), neural cells are connected by AJs containing N-cadherin, and mesenchymal cells are connected by AJs containing N-cadherin and/or cadherin-11. It was therefore a finding of fundamental importance when it was reported that epithelial cells change from exclusively or predominantly E-cadherin AJs to an increased proportion of N-cadherin AJs when they turn into mesenchymal cells as, for example, in early embryogenesis. Similar changes have been reported by many researchers when malignantly transformed cells evade the epithelial cell layer continuity and change their topology to migratory metastatic cells, processes that are often correlated with an increase and often dominance of N-cadherin–based AJs, the "E- to N-cadherin switch" (e.g., Behrens et al., 1989, 1993; Frixen et al., 1991;

Correspondence to Werner W. Franke: w.franke@dkfz.de

Abbreviations used in this paper: AJ, adherens junction; $BS^3$, bis(sulfosuccinimidyl]suberate; IF, intermediate-sized filament; IP, immunoprecipitation; PLC, primary liver carcinoma; RIPA, radioimmunoprecipitation assay.



The Rockefeller University Press $30.00
J. Cell Biol. Vol. 195 No. 5 873–887
www.jcb.org/cgi/doi/10.1083/jcb.201106023

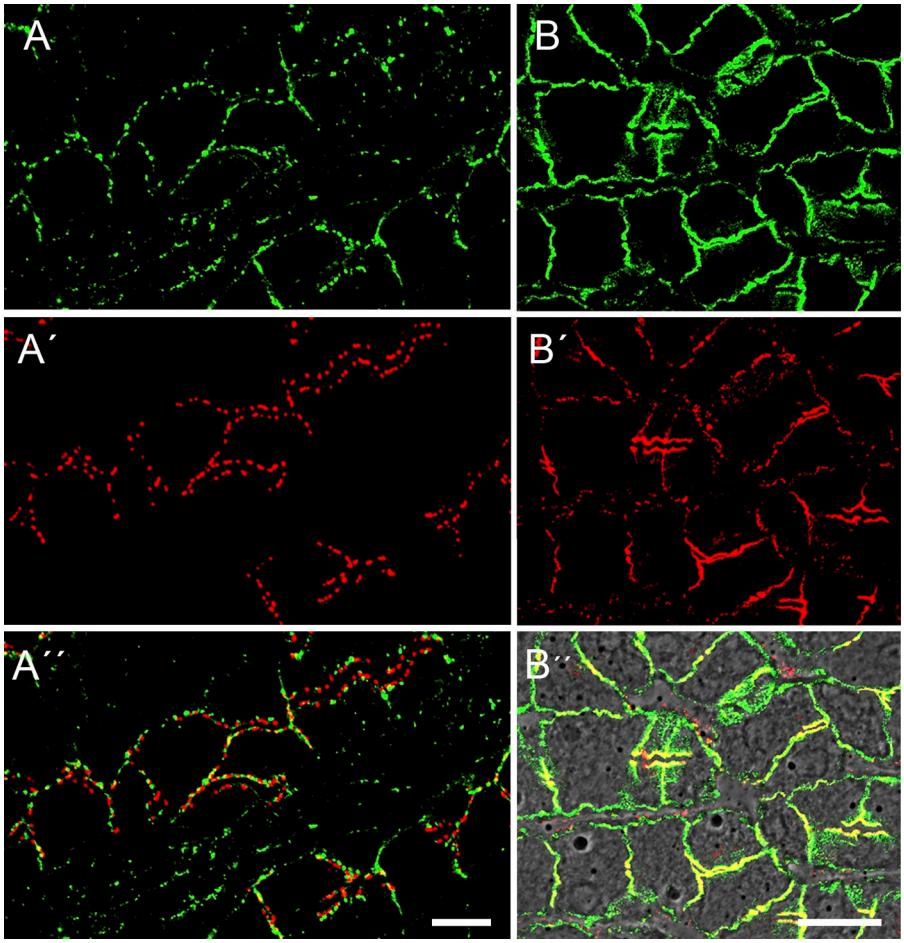


Figure 1. **Identification and localization of the AJ cadherins in mammalian hepatocytes.** (A–B″) Immunofluorescence micrographs of cryostat sections through bovine liver showing double-label reactions of N (A, A″, B, and B″; green)- and E-cadherin (B′ and B″; red), also in comparison with desmosomal junctions (immunolocalizations of desmoplakin are seen as red fluorescent dots in A′ and A″). A different localization of N-cadherin and the desmosomal protein is seen in the double-label immunofluorescence merged color picture (A″), whereas colocalization of N- and E-cadherin is recognized as yellow (merge color)-stained AJ structures (B″; on a phase-contrast background). Bars, 10 µm.

Mareel et al., 1991; Vleminckx et al., 1991; Birchmeier et al., 1993; Takeichi, 1993). Consequently, determinations of E- to N-cadherin changes have become rather generally accepted diagnostic and prognostic criteria of malignancy (e.g., Nieman et al., 1999; Hazan et al., 2000; Maeda et al., 2005; Yilmaz and Christofori, 2009; Berx and van Roy, 2009).

In contrast, over the last two decades, we have observed again and again that in diverse endoderm-derived epithelial tissues and tumors, both E- and N-cadherin coexist in remarkably high, seemingly isostoichiometric amounts and in a close neighborhood. As we have also often noted in high resolution microscopy extensive colocalization of both cadherins in such tissues as well as in cell cultures derived therefrom, we have studied the molecular basis for this apparently antidogmatic phenomenon in greater detail. Here, we report that in diverse endoderm-derived tissues, the vast majority of AJs is based on clusters of heterodimer complexes of E- and N-cadherin in normal tissues as well as in tumors and cell cultures derived therefrom.

## Results

In our research of endoderm-derived tissues, such as liver parenchyma, intra- and extrahepatic bile ducts, gall bladder epithelium, and pancreatic ducts of various mammalian species (human, bovine, porcine, and murine—rat and mouse), and diverse kinds of tumors and cell cultures derived therefrom, we have noted frequent, often predominant cell–cell contact structures positive for both E- and N-cadherin. As this appears to be in provocative contrast to the prevailing concept of a mutually exclusive occurrence of E- and N-cadherin in AJs of such tissues, specifically to the concept of antagonistic functions of these glycoproteins in tumorigenesis, carcinoma invasion, and metastasis, we have examined the AJs of such cells in normal and tumorous tissues as well as in cell cultures in detail.

### Light microscopy of normal and tumor tissues

In cryostat sections of frozen tissues as well as in sections through formaldehyde-fixed, paraffin-embedded tissues microwave treated for antigen retrieval, we consistently noticed densely spaced E- as well as N-cadherin–positive reaction sites along the plasma membranes connecting hepatocytes (Fig. 1, A–A″), including the bile canalicular regions (Fig. 1, B–B″). In some places, these E- and N-cadherin–positive sites could be resolved as linear arrays of punctate structures indicative of AJs (Fig. 1 B). When these arrays of N-cadherin–positive structures were compared by double-label immunofluorescence microscopy, with reaction sites of antibodies specific for desmosomal molecules, they were clearly different, often appearing in linear alternating arrays of AJs and desmosomes along the canalicular plasma membrane (presenting a direct comparison of

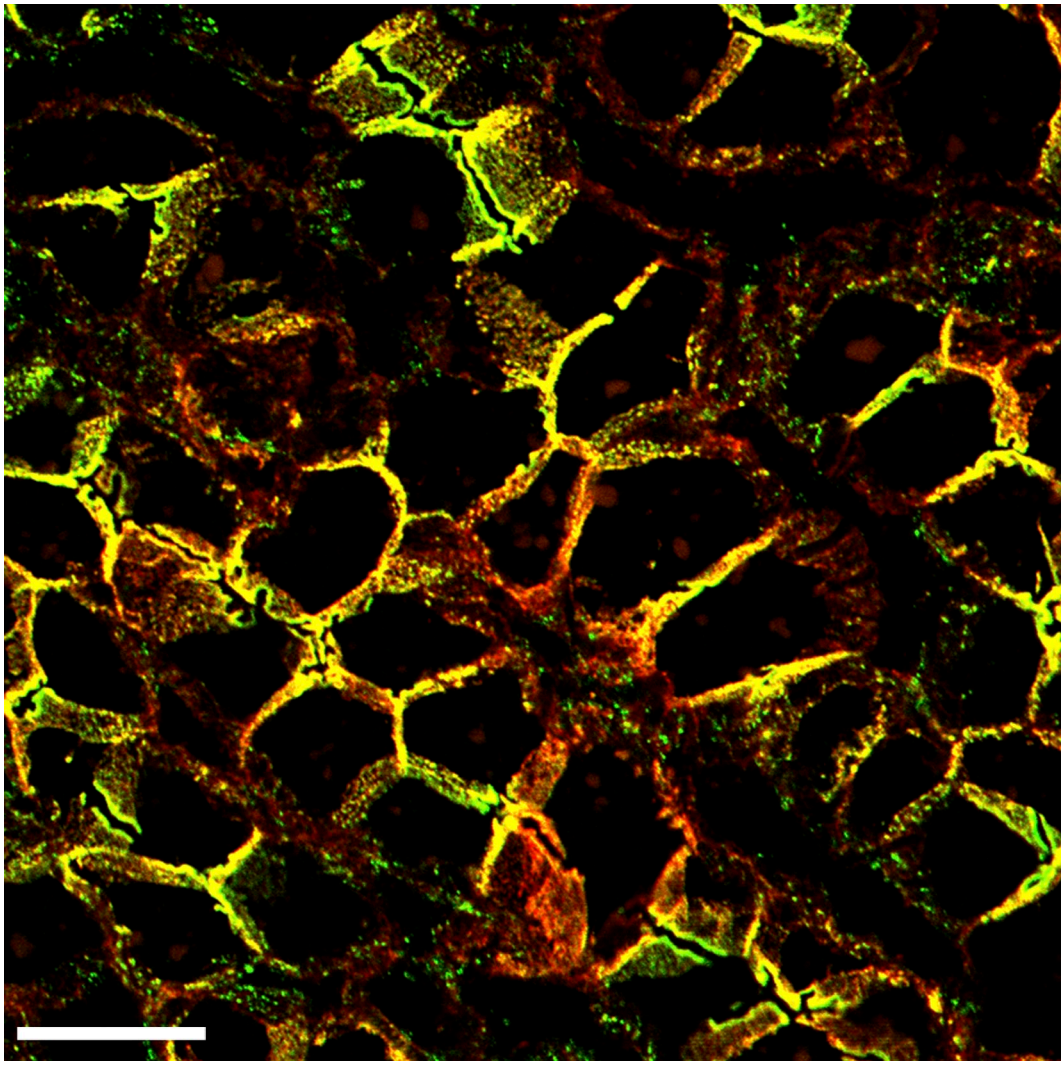

Figure 2. **Identification of structures containing AJs positive for both E- and N-cadherin in plasma membranes of a human hepatocellular adenoma.** Laser-scanning, double-label immunostaining of plasma membranes in a cryostat section through a human hepatocellular adenoma using antibodies specific for E (green)- or N (red)-cadherin (only the merged color picture is presented). Note the colocalization of both cadherins in a high proportion of the tumor cells. Bar, 20 µm.

N-cadherin with desmoplakin; similar results were also obtained for other desmosomal marker molecules, specifically desmoglein Dsg2 and plakophilin Pkp2; Fig. 1, A–A′′). In contrast, in double-label immunofluorescence microscopy comparisons of N- with E-cadherin, far-reaching colocalization was observed (Fig. 1, B–B′′), and this was also often seen in comparisons of N-cadherin with α-catenin, protein ZO-1, and the *armadillo* proteins β-catenin, p120, and p0071 (Fig. S1, A and B). Practically identical results were obtained for all five species examined.

Similar colocalization of E- and N-cadherin in AJ structures was seen in gall bladder epithelium, intra- and extrahepatic bile ducts (Fig. S1, C and D), and pancreatic ducts (Fig. S2), whereas the AJs of the surrounding mesothelium were positive only for E-cadherin (Fig. S1 E shows the absence of N-cadherin in mesothelial cells). Again, essentially identical results were obtained in all five species examined. Colocalization for E- and N-cadherin was also seen in AJ structures of various liver-, gall bladder–, or pancreatic duct–derived tumors as well as in human liver adenomas (Fig. 2), hepato- and cholangiocellular carcinomas, and ductal adenocarcinomas of the pancreas, both in primary and metastatic tumors.

### Microscopy of cell cultures

When monolayer colonies of primary, secondary, and permanent human or rat hepatocyte cultures were examined by double- or triple-label immunofluorescence microscopy, we observed strongly N-cadherin–positive, punctate or even continuously linear-appearing reaction sites in cell–cell contact regions, frequently in perfect colocalization with E-cadherin (Fig. 3, A–B, examples of human cells). Generally, colocalizations of E- and/or N-cadherin were seen with α-catenin, protein ZO-1, and the *armadillo* proteins β-catenin, p120, and p0071. Colocalizations of E- and N-cadherin in AJs as well as with the aforementioned plaque proteins were also frequent in cultures of hepatocellular tumor cells, including permanently proliferative cell lines

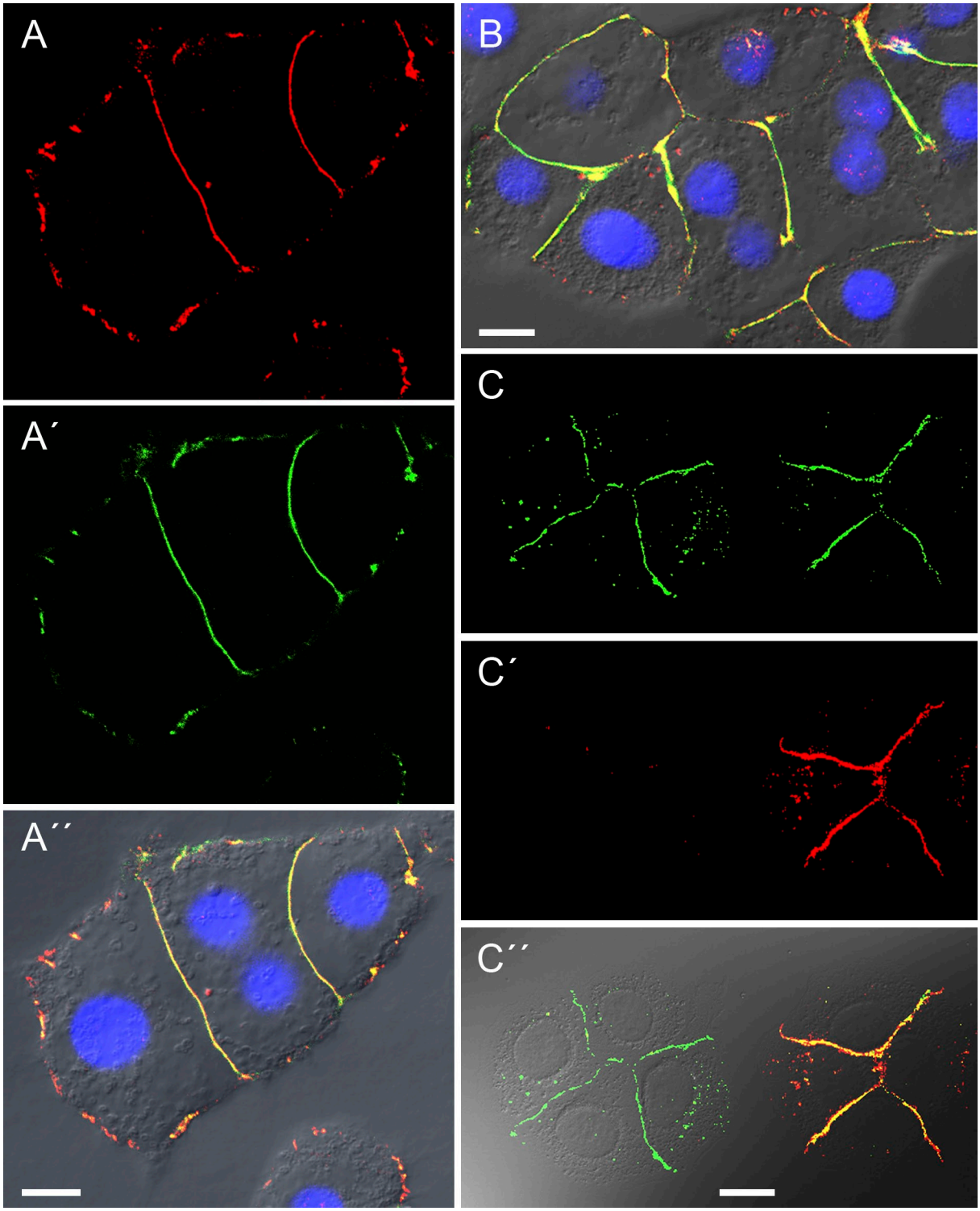


Figure 3. **Identification and localization of E- and N-cadherin–containing AJ structures connecting cells of primary cultures of human hepatocytes and hepatocellular carcinoma cells of line PLC.** (A–C′′) Laser-scanning immunofluorescence microscopy of E–N-cadherin heterodimer–containing AJs in primary human hepatocytes (A and B) or hepatocellular carcinoma cells of the line PLC (C), freshly replated and allowed to reassociate in small colonies, after reaction with antibodies against N (A and A′′, red; C and C′′, green)- and E (A′ and A′′, green; C′ and C′′, red)-cadherin, showing cell–cell contacts with extensive colocalization (yellow merge color; A′′, B, and C′′) in small punctate AJs or in extended linear structures. Note that some colonies show cell–cell contact regions positive for both cadherins and presenting extensive colocalization (A–B; the right hand four-cell colony in C–C′′), whereas other—often directly adjacent—cell colonies present junctions that are positive only for one of the two cadherins (here, N-cadherin on the left of C–C′′). Note also the additional occurrence of small whisker- or dot-shaped structures at the cell surface, which are N- or E-cadherin positive or show already a merged color (yellow). Bars: (A′′ and B) 10 µm; (C′′) 20 µm.

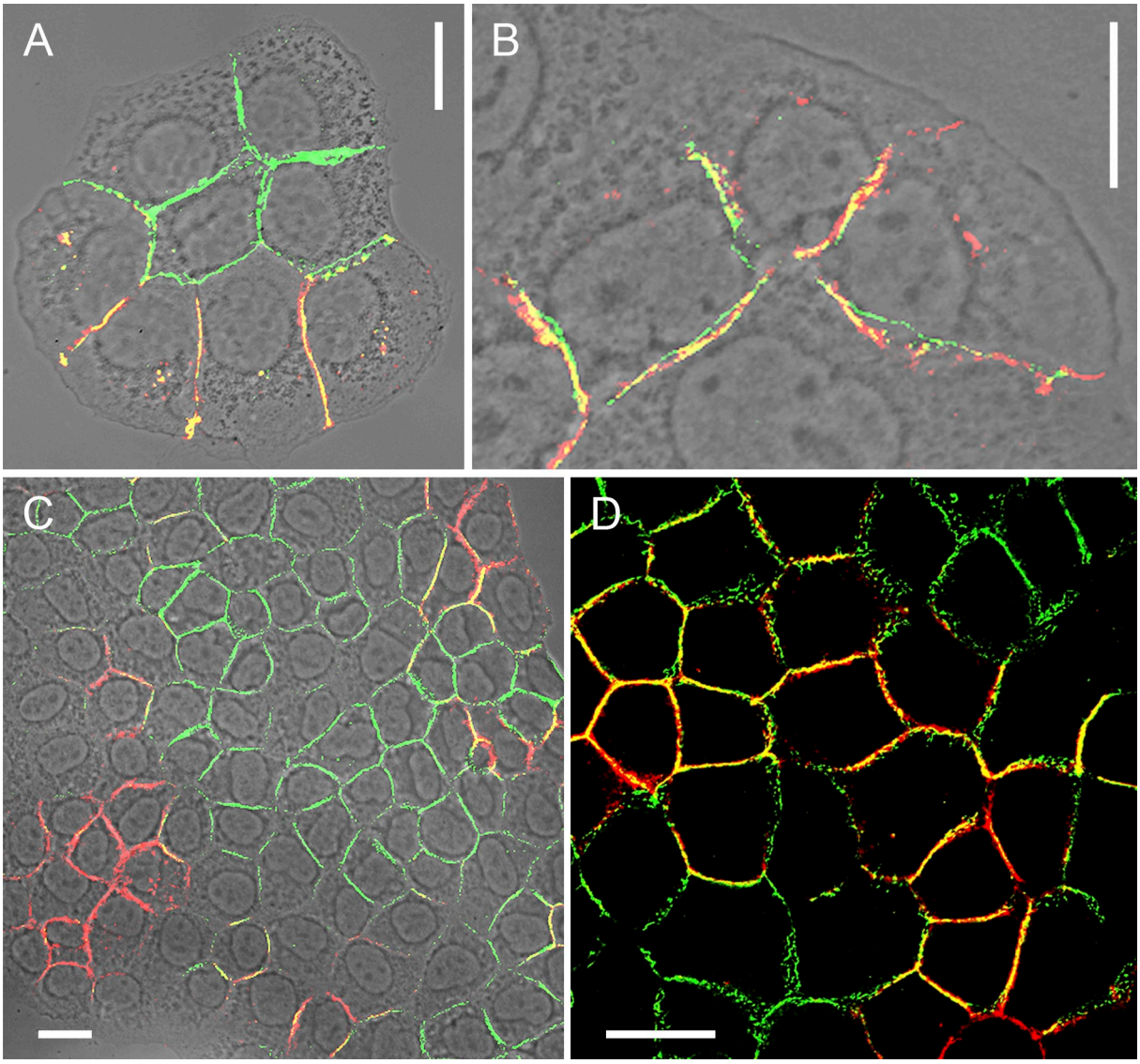


Figure 4. **Marked regional differences of E- and/or N-cadherin–positive AJ structures in cell cultures of hepatocellular carcinoma PLC cells.** (A–D) Laser-scanning double-label immunofluorescence microscopy of reactions with antibodies to N (A, C, and D, green; B, red)- and E (A, C, and D, red; B, green)-cadherin in parts of the same PLC cell colonies, be they small (A and B) or large and near confluent (C and D). (A) Note that in the cell colony the upper portion is positive for N-cadherin only (green), whereas most of the cell–cell contact regions in the lower part of the colony are positive for both cadherins (yellow merge color). (B) Another frequent aspect of N- and E-cadherin colocalization. Close localization presents regions of merged localization (yellow) as well as regions positive for N-cadherin (red) or E-cadherin (green), the latter occurring either in small dots or whiskers or in separate, often quite extended thin zonula-like lines. (C) Dense-grown monolayer cell culture region presenting purely E-cadherin–positive (red circumscribed cells in the bottom left and the top right) or purely N-cadherin–positive (green cell–cell contacts) cells with only some plasma membrane contact regions that show E- and N-cadherin–positive (yellow) merged color cell membranes. (D) More advanced state of E–N heterodimer formation (yellow merge color) in a cell colony (green, N-cadherin; red, E-cadherin), shown at higher magnification and allowing to resolve numerous individual AJs (punctate structures). Bars, 20 μm.

(Figs. 3, C–C′′; 4, A–D; and 5, examples of human liver carcinoma cells of line primary liver carcinoma [PLC]). Such results were also obtained for a series of other human hepatocytic tumor cell lines, such as HepG2, Hep3B, and HuH7, as well as rat hepatocyte and liver carcinoma lines (unpublished data).

In addition, however, and more frequently in freshly trypsinized and replated cell cultures, we noticed small structures appearing as dots, short beaded chains, or whiskers at cell–cell contact sites, on free cell surfaces or on cytoplasmic vesicles, which could appear as positive for either only N-cadherin or E-cadherin or for both (Figs. 3, A–C′′; and 4, A–D). Not infrequently, such small cadherin-positive structures were also positive for one of the aforementioned plaque proteins (unpublished data). And most startlingly, we repeatedly noted cell colonies in which all cell–cell contact regions were densely packed with AJs intensely stained for both E- and N-cadherin, whereas adjacent colonies were characterized by cell–cell contact structures positive for only one of the two cadherins (Fig. 3, C–C′′). And such heterogeneities could also frequently be seen in the same colony, be it small or large (Fig. 4, A–D). The general impression was that in a given cell–cell contact region, one of the two cadherins started AJ formation, whereas the second cadherin appeared somewhat later to associate to heterocomplexes and -structures (Fig. 4, A–D).

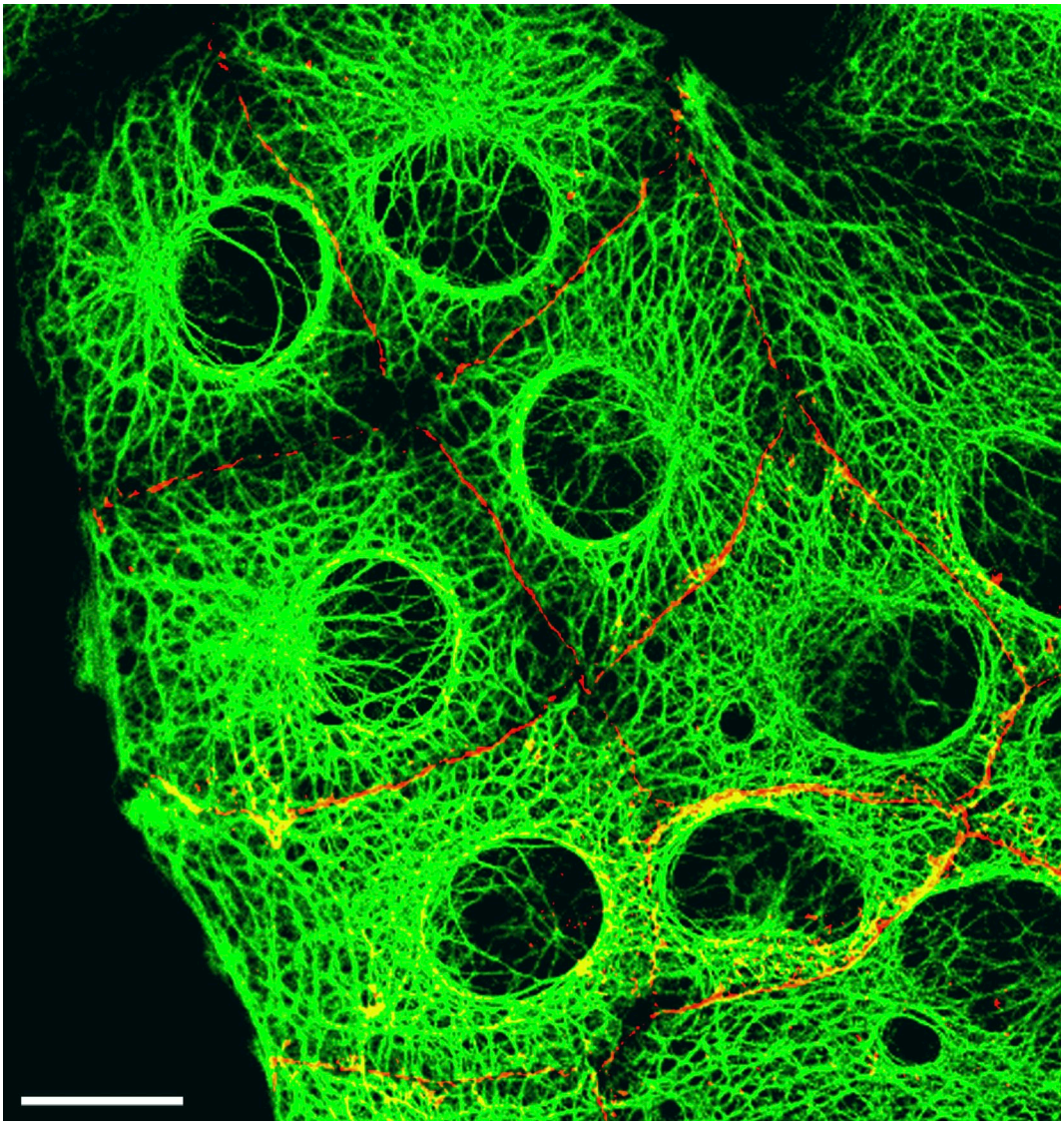

Figure 5. **Advanced state of formation of densely spaced N-cadherin–containing AJs in a culture of human hepatocellular carcinoma cells.** Double-label laser-scanning confocal immunofluorescence microscopy of a reformed PLC monolayer as visualized after reaction with antibodies against N-cadherin (red) located in the numerous, very densely spaced puncta adharentia, which in many regions suggest a continuous AJ structure in a fully developed cytoskeletal system (keratin fibril bundles are shown after reaction with antibodies to keratins 8 and 18; green). Bar, 20 µm.

Finally, in extended, dense-grown monolayer cultures of hepatocytes or hepatocellular tumor cells, characterized by fully developed AJ systems and cytoskeletal filament bundles of the actin microfilament and the keratin intermediate-sized filament (IF) category, we noted high frequencies of AJs positive for both E- and N-cadherin interspersed with desmosomes. Fig. 5 presents an example of an extended, dense-grown PLC cell monolayer with a fully developed keratin IF bundle system, in which apparently all the densely spaced AJs contain N-cadherin in addition to their typical E-cadherin.

### Electron microscopy

In the liver tissues of all five mammalian species examined, the hepatocytes were connected not only by gap and tight junctions, desmosomes, and the canalicular *zonula adherens* but also by numerous rather small, near-isodiametric (30–100 nm) AJs of the puncta adharentia category (Fig. 6, A and B, arrows). Most of these AJs showed rather small, electron-dense cytoplasmic plaques and were interspersed with mostly larger but less frequent typical desmosomes and small junction-free regions (Fig. 6, B–D). Although the plaques of the desmosomes were generally associated with laterally abutting bundles of keratin IFs, the plaques of the punctate AJs were only occasionally resolved to anchor microfilament bundle structures. In systematic evaluations of bovine liver cell structures, almost half (43%) of the lateral contact areas between hepatocytes was occupied by AJs.

Immunoelectron microscopy revealed that by far most, if not all, of these numerous punctate AJs contained not only E-cadherin (Fig. 6 C) but also N-cadherin (Fig. 6 D). Moreover, specific antibodies and preparation techniques allowed us to localize the glycosylated extracellular domains of these cadherins in the intercellular bridges connecting these AJs (Fig. 6 C). These immunolocalization results corresponded with reactions of the specific cytoplasmic plaques positive for the *armadillo*

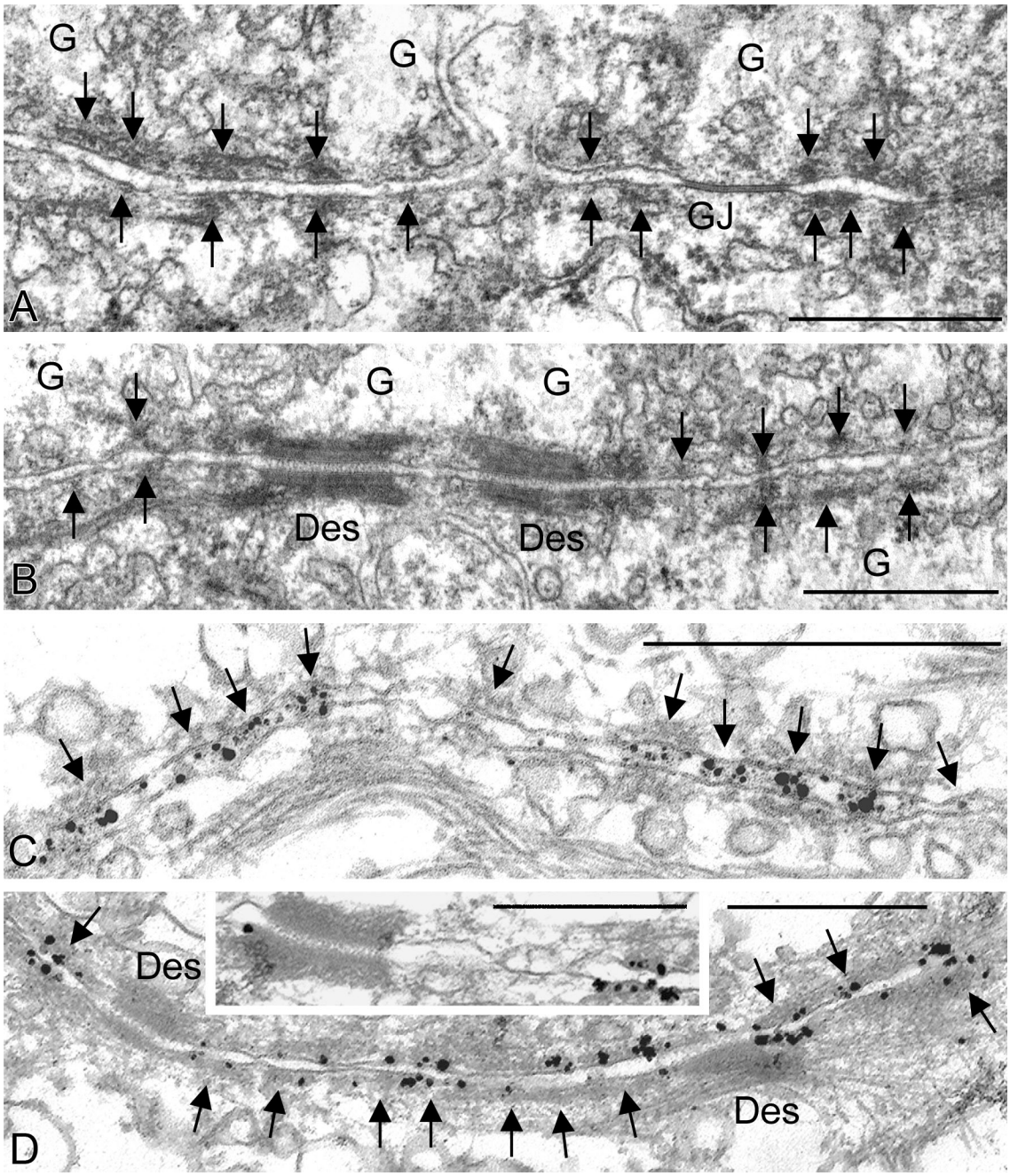


Figure 6. **Electron microscopy of ultrathin sections through bovine liver tissue, showing cell–cell contact regions with high densities of small AJs of the puncta adherentia type that contain E- as well as N-cadherin.** (A and B) Electron micrographs of ultrathin sections showing lateral contact regions of hepatocytes with small but frequent—and for the most part closely spaced—puncta adherentia (denoted by arrows), in comparison with desmosomes (Des) and gap junctions (GJ). G, glycogen aggregate. (C and D) Immunoelectron microscopy of ultrathin sections obtained from cryostat sections and reacted with antibodies specific for E (C)- or N (D)-cadherin shows that most, if not all, puncta adherentia contain both E-cadherin (denoted by arrows; here, the specific epitope is located on the extracellular portion of the molecule) as well as N-cadherin (denoted by arrows; the inset in D also shows a desmosome on the left and an intensely labeled punctum adherens on the right). Bars, 0.5 μm.

proteins β-catenin, p120, and p0071. Immunoelectron microscopic control reactions also showed the specific immunolabeling of the adjacent desmosomes with antibodies to desmoplakin, plakophilin Pkp2, and desmoglein Dsg2 (unpublished data).

### Biochemical analyses

In gel electrophoretic analyses of the proteins of total cells, of cytoskeletal residues, or of plasma membrane fractions enriched in bile canalicular structures (for electron microscopy of such fractions see Franke et al., 1979), N-cadherin was a major protein in liver tissues as well as in cultures of hepatocyte-derived, normal, or malignantly transformed cells (Fig. 7 A presents a series of results). As expected, N-cadherin was also a major protein in cell culture lines of mesenchymal origin, including human hepatic stellate cells of line LI-90 or human glioma cells of line hG-U333 but was totally absent in diverse other epithelial tissues and carcinomas, including several endoderm-derived cell lines, such as human colon carcinoma CaCo-2 cells

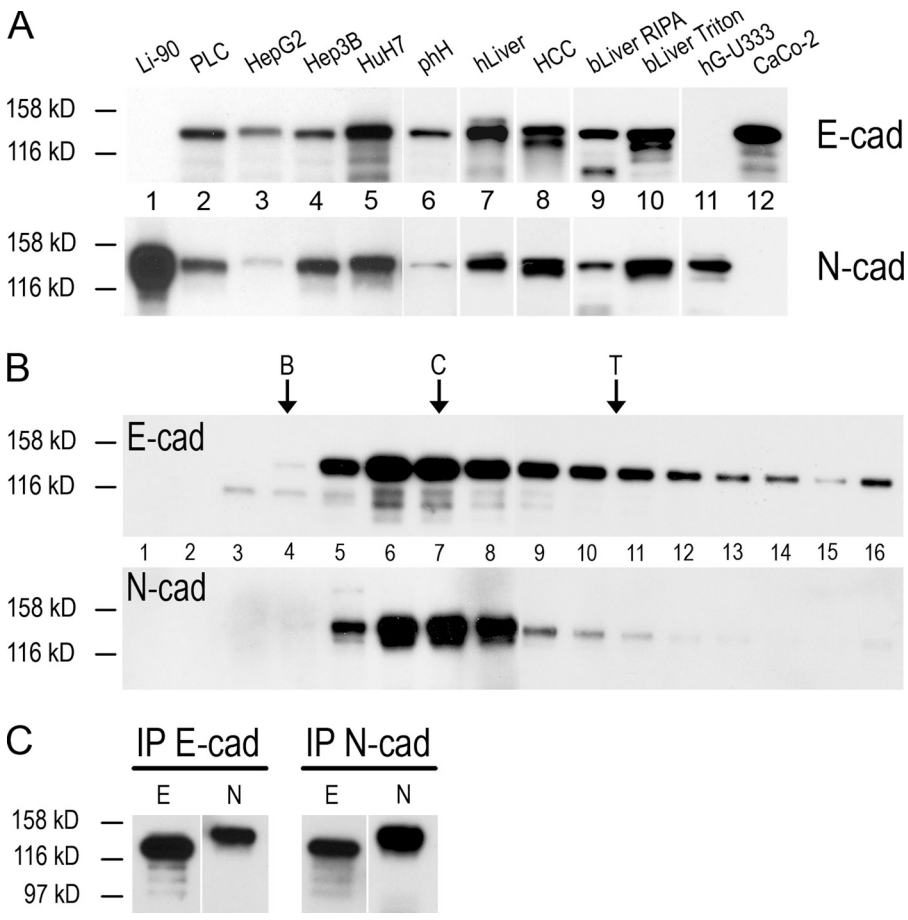


Figure 7. **Immunoblot identification of E- and N-cadherin in the gel-electrophoretically separated polypeptides and protein complexes of whole-cell lysates, sucrose density centrifugation, and IP fractions of mammalian liver tissue and cultured hepatocellular tumor cells.** (A) On SDS-PAGE separation (8% gel) of total proteins, E-cadherin (E-cad) and N-cadherin (N-cad) are detected as distinct bands of ∼135 kD in the following human cells and tissues: hepatocellular carcinoma cells of the line primary liver carcinoma (PLC; lane 2), human hepatoblastoma-derived cells of the line HepG2 (lane 3), human hepatocellular carcinoma cells of the lines Hep3B (lane 4) and HuH7 (lane 5); primary cultures of human hepatocytes (phH; lane 6), human liver tissue (hLiver; lane 7), and a solid human hepatocellular carcinoma (HCC; lane 8). Different detergent-soluble fractions from bovine liver (bLiver; RIPA or Triton buffers; lanes 9 and 10, respectively) have also been analyzed. E-cadherin is not detected in cells of human hepatic stellate cells of line LI-90 (lane 1) and of the human glioma cell line hG-U333 (lane 11) analyzed in parallel but is a major component in cultured cells of the human colon carcinoma line CaCo-2 (lane 12). N-cadherin is detected in all hepatocyte and hepatocyte-derived cells as well as in human hepatic stellate cells of line LI-90 and in the positive controls of human glioma cells (hG-U333) but not in CaCo-2 cells. (B) Sucrose density centrifugation (5–30%) of particles obtained by solubilization of total lysates of PLC cells, followed by fractionation (fraction numbers are given), SDS-PAGE of the fractions obtained, and immunoblotting with antibodies against E-cadherin (top) and N-cadherin (bottom). Note that for both cadherins, the maximum peak is near that of catalase (the positions of proteins analyzed in parallel are given at the top margin: BSA [B] with 4.3 S, catalase [C] with 11.5 S, and thyroglobulin [T] with 16.5 S). (C) Immunoblots of proteins contained in the peak fractions 5–8 of the gradient shown in A and obtained by IP with antibodies to E-cadherin (lane E) or N-cadherin (lane N). Apparent molecular masses according to SDS-PAGE mobility are 135 kD (N-cadherin) and 124 kD (E-cadherin). Molecular masses of reference proteins examined in parallel are indicated on the left. White lines indicate that intervening lanes have been spliced out.

(Fig. 7 A). Liver epithelial cells contained comparable amounts of E-cadherin, which was also found as a major component in CaCo-2 and other colon and colon carcinoma cells but was absent from LI-90 and hG-U333 cell cultures (Fig. 7 A). Remarkably, in most of the total cell lysates or cytoskeletal protein preparations from hepatocyte origin, the silver staining and immunoblot reactions indicated near-isostoichiometric amounts of N- and E-cadherin (Fig. 7 A, lanes 2, 4, 5, and 7–10).

When particles, proteins, and protein complexes obtained from liver tissue or from cultured hepatocyte-derived cells after mild nondenaturing detergent treatments were analyzed by gel filtration chromatography or sucrose gradient centrifugations, the majority of both E- and N-cadherin was recovered in particles of ∼11.5 S and with apparent mean molecular masses of 220–240 kD, which is indicative of heterodimers (Fig. 7 B). When these fractions were subjected to immunoprecipitations (IPs) with antibodies specific for E- or N-cadherin, the peak fractions indeed contained both cadherins in major amounts suggestive of an isostoichiometric ratio (Fig. 7 C).

To test for a possible close neighborhood of the E- and N-cadherin molecules in the cell cultures and tissues positive for both E- and N-cadherin, we exposed preparations of cell fractions, enriched cell particles, or total cytoskeletal residues to various protocols of chemical cross-linking with a wide range of bond bridge distances. Even with the shortest bond distance examined (2.05 Å), i.e., in a reaction with $Cu^{2+}$-phenanthroline to allow the oxidative formation of disulfide bridge bonds, remarkable proportions of both E- and N-cadherin were recovered in covalently linked heterodimer complexes of E- and N-cadherin (Fig. 8, A and B). By exposure to reducing agents, usually DTT or mercaptoethanol, these disulfide bonds could be completely cleaved. Similar covalent heterodimeric complexes were also obtained with other disulfide cross-linkers or with reagents connecting other amino acid residues, including bis(sulfosuccinimidyl)suberate ($BS^3$) as the longest distance (>11 Å) cross-linker applied, which in addition, allowed to obtain even larger cross-link products, up to at least the size of double heterodimers (Fig. 8 C).

### Molecular interference with the formation and stability of E–N heterodimers and AJs

To examine the stability and the dynamics of the E–N heterodimer complexes, we exposed monolayer cultures of cells derived from human hepatocytes and hepatocellular carcinomas

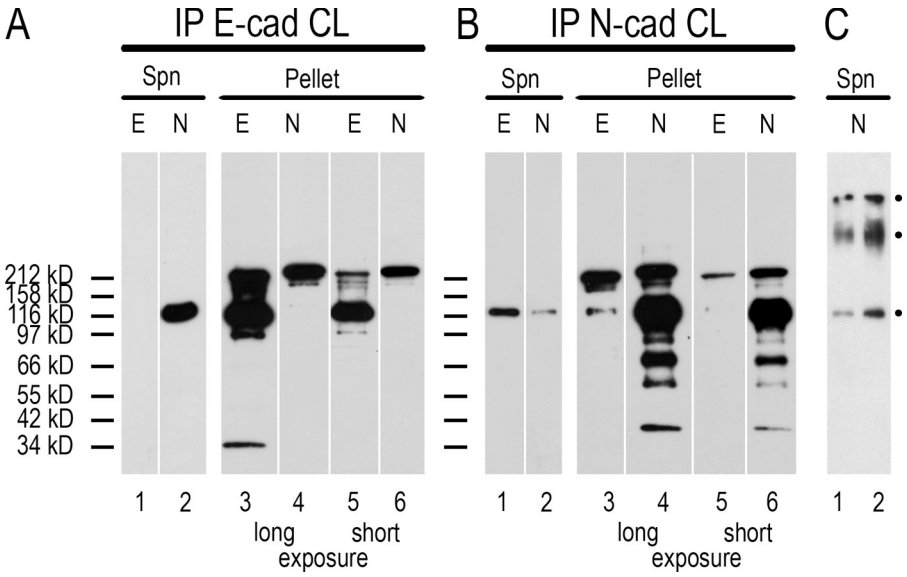


Figure 8. **Identification and characterization of cross-link products of E- and N-cadherin contained in PLC cells and enriched after IP.** (A and B) Total cytoskeletal proteins of PLC cells taken up in RIPA buffer were reacted with cross-link (CL) reagents (in this case oxidative disulfide bridge formation in the presence of $Cu^{2+}$-phenanthroline) and subjected to IP with antibodies to E-cadherin (E-cad; A) or N-cadherin (N-cad; B). The pelleted immunoprecipitates were then analyzed by SDS-PAGE under nonreducing conditions, and polypeptides were identified by immunoblotting using antibodies to E (lane E)- or N (lane N)-cadherin. Spn, remaining supernatant; pellet, material contained in the final sediment. Note that in both kinds of immunoprecipitates the occurrence of a large proportion of E- and N-cadherin in a common polypeptide with an apparent molecular mass of ∼230 kD (molecular mass markers analyzed in parallel are indicated on the left margin). Note also the formation of some proteolytic breakdown products in the specific immunoprecipitates. (C) Cross-link products of higher molecular masses up to ∼450 and >600 kD can be obtained with the very long distance (>11 Å) lysine–lysine cross-link reagent $BS^3$. Positions of major monomeric and cross-linked molecules are marked by dots. White lines indicate that intervening lanes have been spliced out.

to conditions in which the one or the other or both of the two cadherins were drastically reduced or even depleted. In siRNA experiments, Fig. S3, for example, presents the situation at day 3 of exposure of hepatocellular carcinoma cells of line PLC to siRNAs interfering with E-cadherin, N-cadherin, or with both. When the level of E-cadherin was reduced, the level of N-cadherin was only slightly affected, and the reverse was found in experiments interfering with mRNA encoding N-cadherin. In striking contrast, interfering with mRNAs for both cadherins (Fig. S3, lane 3) led to very dramatic reductions of both E- and N-cadherin. Interestingly, in such experiments, the levels of the *armadillo* proteins (Fig. S3, β-catenin) were only moderately reduced. When the times of exposure to media containing these siRNAs were prolonged for a further 1 d, only very minor residues of the specific cadherins were detected.

In such mRNA interference experiments using siRNA for E- or N-cadherin or mixtures of both, the state of cell–cell adhesion was also routinely examined by immunofluorescence microscopy in combination with phase or interference contrast optics (Fig. 9 presents results obtained at the end of day 3). When one of the two cadherins was markedly reduced or even appeared completely depleted, the monolayer organization remained—by and large—in close cell–cell contact mediated by "normal" homodimer cadherin complexes (Fig. 9, A–H). Control experiments revealed the presence of desmosomes, tight junction, and gap junction connections in such cell colonies.

Drastic changes, however, were noted in the cell culture colonies treated with both siRNAs, i.e., after drastic reduction of both E- and N-cadherin. Here, only some residual, irregularly shaped cell colonies were seen, which presented the AJ plaque proteins still in continuous zonula adherens–like structures extending along the remaining cell–cell contact regions (Fig. 9, I and J) or—in a more advanced state of AJ disintegration—as long curvilinear bands containing the plaque proteins, which were translocated deeper into the cytoplasm (Fig. 9, J–M, protein ZO-1). As these structures of detached plaques resembled, in both light and electron microscopy, very much the cytoplasmic AJ belt retraction aggregates known from exposures of epithelial cell cultures to media of reduced $Ca^{2+}$ contents (e.g., Kartenbeck et al., 1982), we also performed such experiments with low $Ca^{2+}$ media or with 2 mM EGTA and obtained very similar results (unpublished data). Remarkably, in such cell colonies, the appearance of AJ plaque retraction belts was accompanied by both the retention of some E- or N-cadherin at the plasma membrane amino acids well as the formation of cadherin-containing structures in the cytoplasm (Fig. 9, J–M), which on electron microscopic examination, were revealed as clusters of vesicles (compare Kartenbeck et al., 1982; Le et al., 1999; Akhtar and Hotchin, 2001; de Beco et al., 2009; Hong et al., 2010).

## Heterotypic trans-connections between E–N-cadherin heterodimer and N-cadherin homodimer AJ

When we examined the possibility that E–N-cadherin–based complexes of epithelial cell AJs might also stably attach to other kinds of cadherin AJs in cell culture experiments, we found that the E–N-cadherin AJs of hepatocyte-derived cell cultures were able to form direct heterotypic junctions with the pure N-cadherin AJs of various mesenchymally derived cells. For example, we show a mixed culture of hepatocellular PLC cells confronted with transformed fibroblasts of line SV80 (known to form only N-cadherin AJs; Rickelt et al., 2009). Clearly, such epithelial cells are able to establish numerous new junctions connecting the epithelial E–N heterodimer AJs with the purely N-cadherin–containing AJs of the fibroblasts (Fig. 10, B and C). Similar results were obtained in confronting cultures of other hepatocyte-derived normal and tumorous cells with diverse fibroblastoid and myoid cell types. It is also not unlikely that

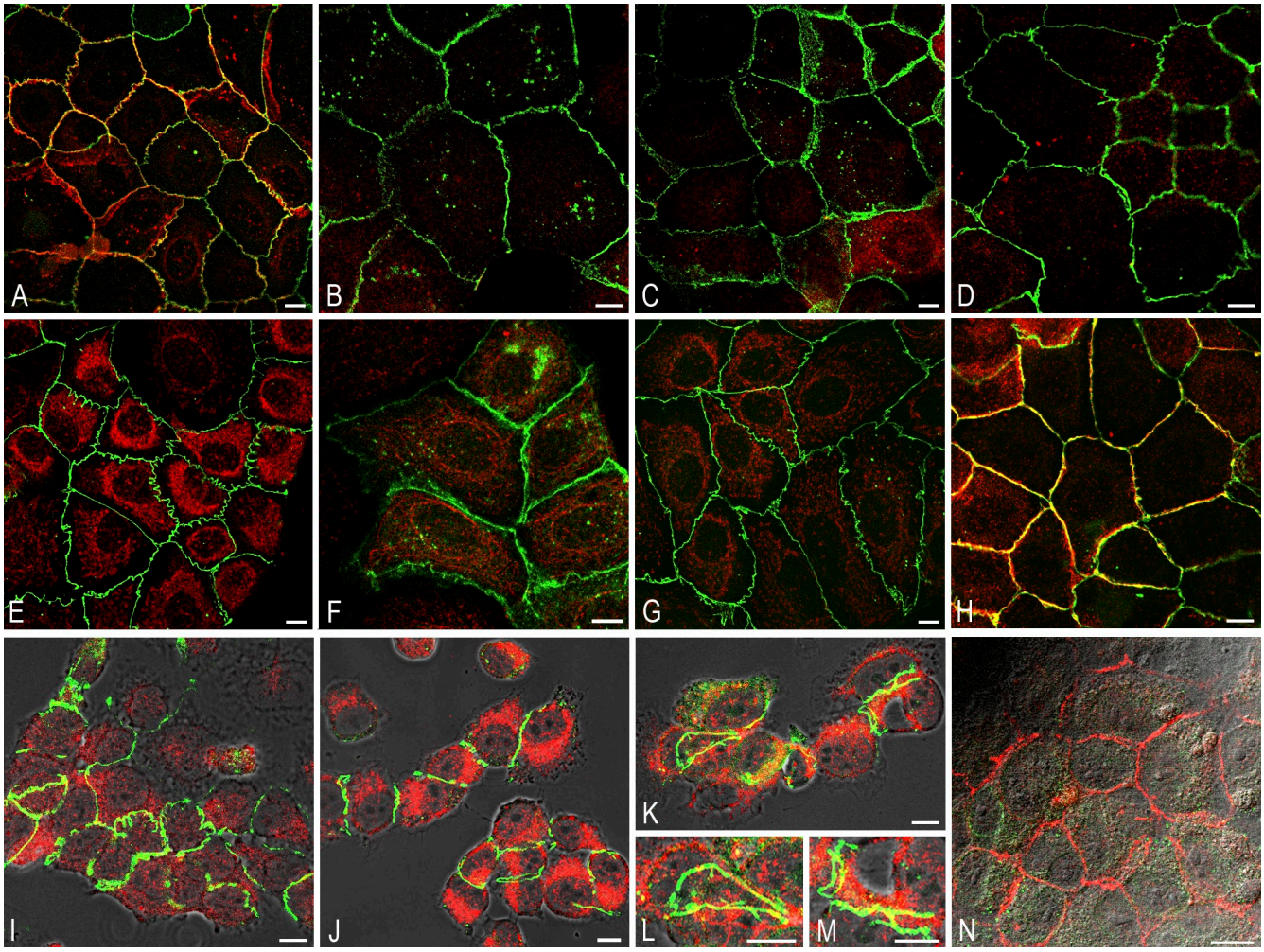


Figure 9. **Changes of structure and composition of AJs upon treatment of monolayer cultures of human hepatocyte-derived (PLC) cells with siRNAs interfering with mRNAs encoding different cadherins.** (A–N) Laser-scanning double-label immunofluorescence microscopy of monolayer cultures of PLC cells treated with siRNA interfering with mRNA encoding E-cadherin (B–D) or N-cadherin (E–H) or with both siRNAs (I–M), in comparison with control cultures without siRNA added (A) or treated with siRNA interfering with nuclear lamins A and C (N). Results of treatments for 72 h, with one change of siRNA-containing medium after 24 h, are shown. (A) Densely grown PLC cells immunostained here for N-cadherin (red) and plaque protein ZO-1 (green). Note the extended cell–cell contact regions stained for one of the two markers or in yellow merged color. (B–D) Cells treated with siRNA interfering with E-cadherin show exclusively the N-cadherin reaction in their cell–cell contact regions (B and C, green), whereas only occasionally, some indistinct E-cadherin (red) fluorescence is seen in the perinuclear cytoplasm (C; e.g., cell on the bottom right). All cell–cell contact regions are also positive for all AJ plaque markers as shown, for example, for protein ZO-1 (D, green). (E–H) Upon treatment with siRNA interfering with mRNA encoding N-cadherin, cell–cell contact regions are intensely stained for E-cadherin (green), whereas only very little and faint residual N-cadherin (E–G, red), mostly in endocytotic vesicles, can still be seen in the cytoplasm (F and G). The AJ plaque proteins are continually present (G; e.g., protein ZO-1 is shown in green). The cells are obviously still kept in contact by AJs based on E-cadherin alone (H, red), which is closely associated with the AJ plaque proteins (green; protein ZO-1 in H), as indicated by yellow merge color. (I–M) When the cell cultures are exposed to both, i.e., siRNA interfering with E-cadherin mRNA and siRNA interfering with N-cadherin mRNA, some remaining cell colonies, although mostly smaller, are still recognized that are not demonstrably positive for E- or N-cadherin but in which extended AJ-type contacts are seen that are still positive for AJ plaque proteins, such as protein ZO-1 (green). In contrast, some residual cadherins (E-cadherin is shown in red immunofluorescence) are demonstrable only deep in the cytoplasm, often recognizable as distinct dotlike endocytotic vesicle structures or still in association with the extended AJ plaque-derived cytoplasmic bands positive for protein ZO-1 (green bands in K, L, and M) and other plaque proteins (not depicted; for details of the formation and organization of such zonula adherens–like AJ plaque-derived structures see Kartenbeck et al., 1982). (N) Control cell culture treated in parallel with siRNAs to lamins A/C but reacted with antibodies for E-cadherin (red) and nuclear lamins A/C (green) to demonstrate the stability of the cell monolayer cultures in such experiments. The cells are connected by normal-looking extended AJ structures positive for E-cadherin. Positivity of the latter structures for N-cadherin has also been seen in parallel experiments. In contrast, no nuclear lamina decorated by lamin A/C immunofluorescence is seen. Bars, 10 µm.

the heterotypic coupling of the AJs of cultured chick hepatocytes to cultured chicken eye lens cells reported by Volk et al. (1987), interpreted as E- to N-cadherin adhesion, might have been based on the coupling of hepatocytic E–N-cadherin dimers to lens N-cadherin. Heterophilic binding of E- to N-cadherin with remarkable adhesion strength has more recently also been demonstrated in transfected CHO cell cultures (Katsamba et al., 2009).

## Discussion

Our results demonstrate the presence of large amounts of both E- and N-cadherin in diverse endoderm-derived epithelial cells, including hepatocytes, i.e., probably the biochemically most studied mammalian cell type, as well as bile, pancreatic duct epithelia, and gall bladder epithelium. Large, but often regionally

varying, amounts of both cadherins are also found in the corresponding pathologically altered epithelial systems of adenomas and carcinomas and also in diverse kinds of cultured cells derived from such tissues and tumors. Moreover, in most of the cell types examined, these two classical cadherins occur in near-isostoichiometric proportions, and this appears to be readily explained by our finding that a very large proportion of these molecules occurs in the form of E–N heterodimers clustered into AJs connecting such cells.

Formations of cis-homodimers of either E- or N-cadherin have previously been reported in various epithelial systems (e.g., Adams et al., 1998; Chitaev and Troyanovsky, 1998; Yap et al., 1998; Wheelock and Johnson, 2003; Perez and Nelson, 2004; Gumbiner, 2005; Troyanovsky, 2005; Shapiro and Weis, 2009; Zhang et al., 2009). Cis-homodimer E-cadherin complexes have also been shown to assemble upon cotransfections of cDNA constructs into AJ-free nonepithelial cells (Takeda et al., 1999; Ozawa, 2002; Takeda, 2004), whereas heterodimer cadherin complexes have so far only been reported to form between N- and R-cadherin upon transfection of mouse fibroblastoidal L cells with specific cDNA constructs (Shan et al., 2000). These authors have further emphasized that in their experiments, E-cadherin could not at all dimerize with N-cadherin, similar to the study of Johnson et al. (1993) that in cells containing E-cadherin together with P-cadherin, these two glycoproteins segregate into strictly separate homodimers. On the other hand, Duguay et al. (2003) and Foty and Steinberg (2005), also using L cell transfections, have described heterotypic cadherin adhesion complexes of various kinds controlling cell sorting but have not determined the specific biochemical nature of the complexes formed.

Surprisingly, the abundance of stable heterodimers of N- and E-cadherin in normal and malignantly transformed hepatocytes—both in tissues and in cell cultures—has hitherto escaped detection, probably because of methodological reasons. Obviously, it is difficult to relate our observations in hepatocytes and hepatocyte-derived tumor cells to those reported by previous authors who have either seen only E-cadherin (e.g., Ihara et al., 1996) or have mentioned the additional occurrence of a special cadherin, called hepatocyte N-related cadherin, at certain lateral plasma membranes but not at all at canalicular membranes or in bile duct epithelial cells (Kozyraki et al., 1996). Moreover, these authors have reported that the hepatocyte N-related cadherin occurs only in a portion of the hepatocellular carcinomas, whereas a much lower proportion of carcinomas contain only N-related cadherin but no E-cadherin. Nuruki et al. (1998) have reported immunostaining reactions for both E- and N-cadherin in human hepatocytes, whereas in many hepatocellular carcinomas, E-cadherin but not N-cadherin is markedly displaced. Again, differently, Doi et al. (2007) have described that in adult mouse liver, E- and N-cadherin do not show the same distribution but rather a mutually exclusive pattern in different zones of the liver lobules. According to Tsuchiya et al. (2006), E- and N-cadherin immunostaining can be seen along plasma membranes of hepatocytes and bile duct epithelium but not in pancreatic ducts. And recently, Govindarajan et al. (2010) have reported the absence of N-cadherin in early cultures of rat

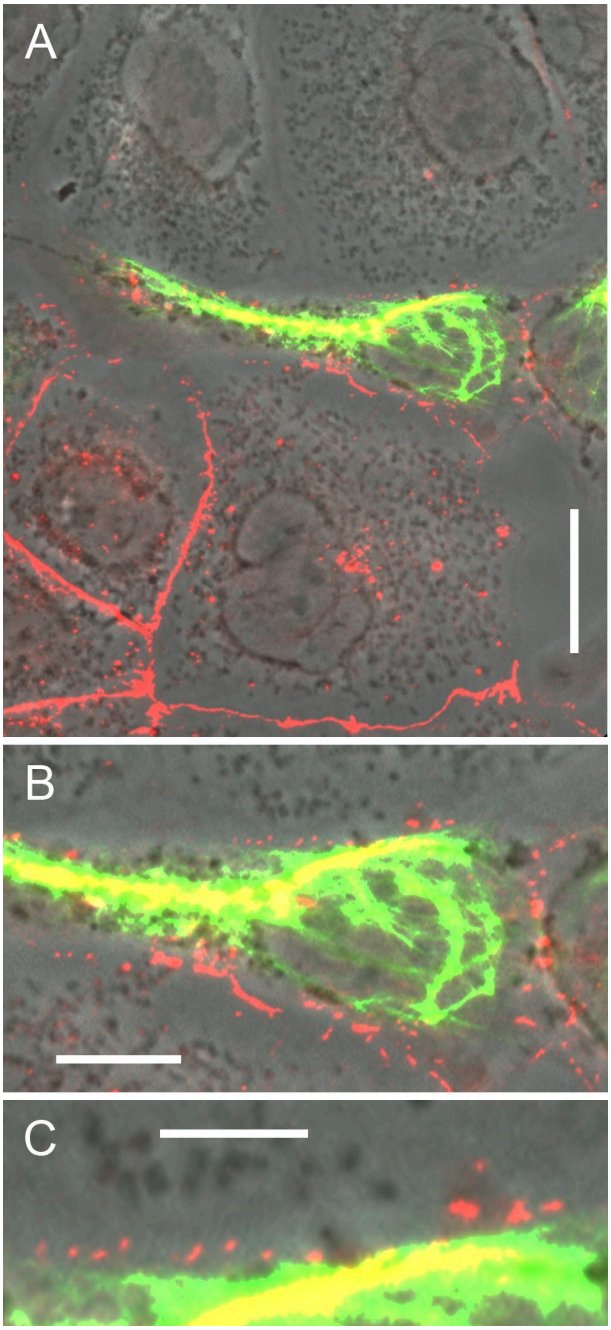


Figure 10. **Localization and characterization of N-cadherin–containing heterotypic AJ structures connecting human fibroblasts and hepatocellular carcinoma cells of line PLC.** (A–C) Laser-scanning, double-label immunofluorescence microscopy (on a phase-contrast basis) of co-cultures of freshly dispersed transformed human fibroblasts (shown here is line SV80) and hepatocellular carcinoma cells of line PLC in a mixed cluster cell colony grown to confluency, after reaction with antibodies against N-cadherin (red) and the IF protein vimentin (green) as a marker of the fibroblasts. Punctate AJs containing N-cadherin occur not only as homotypic junctions formed between SV80 fibroblasts but also as heterotypic structures connecting N-cadherin AJs of fibroblasts and E–N-cadherin heterodimers of AJs of adjacent PLC cells. In the latter, the AJs are also positive for E-cadherin. Shown here are an overview (A) and details presenting special clarity at higher magnification (B and C), the latter allowing the resolution of an array of at least eleven variously sized AJ structures (red dot structures) connecting a fibroblastoid with a hepatocyte-derived cell. The yellow-stained structures are N-cadherin AJs located on the bottom side of the cells. Bars: (A) 20 µm; (B) 10 µm; (C) 5 µm.

liver epithelial cells, but they have also noted its appearance after several passages. In these studies, distinct molecular structures have not been identified as colocalization sites of E- and N-cadherin.

For about two decades, relative frequencies and immunohistochemical reaction intensities of N- versus E-cadherin have been widely used as predictive criteria in pathology, liver tumor pathology included (e.g., Wei et al., 2002; Inayoshi et al., 2003; Cho et al., 2008). Generally, the increase of N- over E-cadherin in the so-called epithelial–mesenchymal transition cadherin switch is generally taken as a diagnostic indicator of the invasive and metastatic potential of a given carcinoma (e.g., Nieman et al., 1999; Ochiai et al., 1999; Hazan et al., 2000; Kim et al., 2000; Cavallaro and Christofori, 2004; Wheelock et al., 2008; Kalluri and Weinberg, 2009; Thiery et al., 2009). We now propose to use the identification of E–N-cadherin–positive AJs and, in particular, E–N-cadherin heterodimers as a diagnostic cell-type marker for the origin and nature of a given kind of tumor, which might be of special value in cases of distant metastases of carcinomas derived from liver, bile tract, or pancreatic duct.

Finally, our discovery of heterodimeric E–N-cadherin complexes in the AJs of a special category of endoderm-derived cells should also enforce a general reconsideration of the cadherin switch hypothesis of carcinogenesis. Apparently, a remarkable level of promiscuity of different cadherins is tolerated in some of the endoderm-derived cell types and functions (e.g., Niessen and Gumbiner, 2002; Capaldo and Macara, 2007; Kan et al., 2007). On the one hand, the lack of E-cadherin, for example in hepatocytes and intestinal cells, or its complete exchange by N-cadherin has been found to interfere with specific functions and morphogenic processes and may even result in pathogenic developments (e.g., Théard et al., 2007, 2008; Libusova et al., 2010). Our study now suggests that the formations, maintenance, and functions of E–N heterodimer AJs may define a special epithelial differentiation pathway of normal development as well as in tumor formation and progression. In particular, we think that our observations of E–N heterodimer–mediated coupling of epithelial and carcinoma cells with diverse kinds of mesenchymal cells should lead to general studies of cell–cell interactions in development and tumor growth, notably metastasis, as well as to the design of special therapeutic anticarcinoma cytostatic peptide or other drugs of the N-cadherin interference category (Blaschuk and Devemy, 2009). And finally, our alarming finding that carcinoma cells equipped with E–N heterodimer AJs can directly and stably attach to N-cadherin AJs of stromal cells will certainly lead to a reconsideration of the cell biological basis of tumor–stroma relationships.

## Materials and methods

### Tissues and cultured cells

Liver and pancreas tissues of bovine and porcine origin were obtained freshly in a local slaughterhouse, and murine (mouse and rat) tissue samples were obtained from the animal houses of the German Cancer Research Center, the National Center for Tumor Diseases Heidelberg, and Hannover Medical School. Cryopreserved human tissue samples, provided by T. Longerich and E. Herpel (National Center for Tumor Diseases, Heidelberg, Germany), included nontumorous liver tissues of partial hepatectomies from liver metastases of colorectal cancer as well as normal pancreas and gall bladder. Tumor samples were cryopreserved or formaldehyde fixed and paraffin embedded (e.g., Straub et al., 2008). For biochemical experiments, tissue samples were either directly used or frozen in liquid nitrogen and kept at −80°C until use. In parallel, human and rat hepatocytes were isolated and prepared as suspensions of cells or grown in cell culture.

Human adult hepatocytes were isolated as previously described (e.g., Alexandrova et al., 2005) using a modified three-step collagenase perfusion from surgical resectates (obtained from patients with informed consent). Primary adult murine (rats and C57BL/6 mice) hepatocytes were isolated by a two-step collagenase perfusion method originally described by Seglen (1979) with minor modifications. Perfusion solutions were introduced into the tissue through catheters placed into the portal or hepatic vein branches. After the digestion phase, the liver tissue was manually disrupted with sterile scissors and scalpels. To separate undigested tissue pieces, the suspended hepatocytes were passed through 750- and 500-µm filters into 50-ml tubes (Falcon; BD).

Primary and secondary cultures of normal human, rat, and mouse hepatocytes, permanently growing human hepatocellular tumor lines, such as PLC, HepG2, Hep3b (obtained from the American Type Culture Collection), and HuH-7 (JTC-39; Japanese Collection of Research Bioresources Cell Bank, Okayama University), as well as primary cells and various lines of rat hepatocytes (e.g., CRL-1439, clone 9; American Type Culture Collection) and hepatoma cells were allowed to grow on glass coverslips coated with 0.01% collagen or 0.005% fibronectin essentially as previously described (e.g., Borenfreund et al., 1980; Franke et al., 1981b; Kern et al., 2002). Human hepatic stellate cells of line LI-90 were grown in DME containing 10% fetal calf serum (Higashi et al., 2004). Primary murine hepatocytes growing in culture were prepared from healthy mice anesthetized. Here, the liver was perfused through the vena cava, first with liver perfusion medium for 15 min at 37°C and thereafter with a solution containing collagenase type IV (Roche) for 8 min at 37°C, before they were taken up and grown in Williams' medium E. For comparison, we also used the human colon carcinoma lines CaCo-2, Colo320DM, and HT29Glu, pancreatic adenocarcinoma cells of the lines Panc-1 and Capan-1, and human glioma cells of line hG-U333CG/343MG.

For analyses of proteins of AJs, mostly bovine and murine liver tissues or bile canalicular fractions were used (e.g., Franke et al., 1979, 1981a; see also Yamazaki et al., 2008) as well as cultures of various hepatocellular carcinoma cells grown in media containing different $Ca^{2+}$ concentrations (compare Duden and Franke, 1988; Kartenbeck et al., 1991; Demlehner et al., 1995).

### Antibodies and reagents

Primary antibodies used in this paper are listed in Table S1. Secondary antibodies used were Alexa Fluor 488– and 594–coupled mouse and rabbit antibodies (MoBiTec) as well as the specific Cy3- and Cy5-coupled mouse, rabbit, or guinea pig antibodies (Dianova). For immunoblot analysis, horseradish peroxidase–conjugated secondary antibodies were applied (Dianova).

### Immunocytochemistry

Tissue cryosections were air dried for ≥1 h and then fixed in acetone for 10 min at −20°C. Liver, gall bladder, and pancreas tissue specimens were, in most cases, preincubated with PBS containing 0.2% Triton X-100 for 5 min followed by exposure to primary antibodies in PBS for 30 min each, two washes in PBS for 5–10 min each, and exposed to the specific secondary antibodies for 30 min. After two 5–10-min washes in PBS, the cell preparations were rinsed in distilled water, fixed for 5 min in ethanol, and mounted in Fluoromount G (Biozol Diagnostica).

The cell suspensions were centrifuged at 50 *g* for 10 min, and the cell pellets were resuspended in ice-cold buffer. An aliquot of the cell preparations was separated for cell counts and viability analyses (phase-contrast microscopy and trypan blue exclusion test). For all experiments, suspensions with >85% of viable hepatocytes were used. The nonhepatocyte fraction, including leukocytes and nonparenchymal liver cells, in the cell suspension was <5% (microscopic analyses). Plating efficacy of the hepatocytes on collagen-coated cell-culture dish surfaces exceeded 80% in all preparations. Primary and secondary rat hepatocytes were isolated and grown on coverslips essentially as previously described for liver and other cell cultures (e.g., De Smet et al., 1998; Peters et al., 2010; Franke and Rickelt, 2011).

### Immunofluorescence microscopy

Immunofluorescence microscopy of cell cultures and of sections through formalin-fixed, paraffin-embedded tissues was performed as previously described (e.g., Straub et al., 2003, 2008; Rickelt et al., 2009). Therefore, cells grown on glass coverslips were briefly rinsed in PBS and fixed for 5 min either with 2% formaldehyde in PBS at RT or in methanol (5 min) followed by acetone (20 s), both at −20°C. The samples were then briefly air dried and rehydrated in PBS just before the immunostaining procedure. After permeabilization in 0.2% Triton X-100 for 5 min, cells were washed several times in PBS. Primary antibodies were applied for 1 h at RT followed by three washes in PBS (5 min each), an incubation with secondary antibodies (30 min at RT), washing with PBS (3× 5 min), a short rinse in distilled water, and finally, dehydration in 100% ethanol (1 min). After air drying, specimens were mounted with Fluoromount G. Epifluorescence was documented with a photomicroscope (Axiophot; Carl Zeiss) equipped with a camera (AxioCam HR; Carl Zeiss) as well as Plan Neofluar 63×/1.25 NA oil and Plan Neofluar 40×/1.30 NA oil objectives. For confocal laser-scanning immunofluorescence microscopy, a microscope (LSM 510 Meta; Carl Zeiss) equipped with Plan Apochromat 63×/1.40 NA oil and Plan-Neofluar 40×/1.30 NA oil objectives was used. AxioVision Release 4.6.3.0 and LSM Image browser 3.2.0.115 software (both obtained from Carl Zeiss) was used for image processing, and Photoshop CS3 (Adobe) was used for final figure preparation.

### Electron and immunoelectron microscopy

For ultrathin section experiments, liver, gall bladder, or pancreas tissue pieces of human, bovine, porcine, or rodent origin were fixed with 2.5% glutaraldehyde in 50 mM sodium cacodylate buffer, pH 7.2, containing 50 mM KCl and 2.5 mM $MgCl_2$, for 30 min, washed three times in the same buffer, postfixed with 2% $OsO_4$ in 50 mM cacodylate buffer for 2 h, and repeatedly washed in this buffer. Thereafter, the tissue blocks were stained overnight with 0.5% uranyl acetate in water, washed, dehydrated, and embedded in Epon. Ultrathin sections were poststained with lead (Franke et al., 1979).

For immunoelectron microscopy, ∼5-µm-thick cryostat sections were fixed with 2% formaldehyde in PBS for 10 min, rinsed three times for 5 min each with PBS containing 50 mM $NH_4Cl$ to quench residual-free aldehyde groups, and then treated with 0.1% saponin in PBS for 5 min followed again by several PBS washes. Primary antibodies were applied for 1 or 2 h followed by three washes with PBS for 5 min. As secondary antibodies, goat anti–mouse or anti–guinea pig immunoglobulins coupled to particles (Nanogold; Biotrend) were applied for 2 h or longer. Specimens were then washed with PBS, briefly fixed with 2.5% glutaraldehyde (5, 10, or 15 min), and rinsed with cacodylate buffer followed by rinses with Hepes buffer, pH 5.8, containing 200 mM sucrose. The primary gold particles bound were then silver enhanced using a silver enhancement kit (HQ Silver; Biotrend) for 3–6 min. Enhancement was stopped with 50 mM Hepes buffer containing 250 mM sodium thiosulfate, and specimens were washed with distilled water and postfixed with 2% $OsO_4$ for 30 min, dehydrated, and embedded in Epon. Ultrathin sections were prepared with an ultramicrotome (Reichert Jung; Leica). Electron micrographs were taken at 80 kV using an electron microscope (EM 910; Carl Zeiss; compare Rickelt et al., 2009).

### Fractionations of cell junction components

Small tissue blocks were taken up in SDS sample buffer (250 mM Tris-HCl, pH 6.8, 2% SDS, 10% glycerol, and 125 mM DTT) or IP buffer (see Gel electrophoresis, IPs, and immunoblotting) and homogenized with a homogenizer (Dounce or Potter-Elvehjem; Braun). To obtain total cell lysate proteins, tissues or cultured cells were directly homogenized in SDS sample buffer for particle fractionations, and the proteins of the pelleted material of the fractions of interest were analyzed as described in the following paragraph. For preparations of cytoskeletal fractions from confluent cell cultures, cells were washed with ice-cold PBS, incubated in low salt buffer containing 10 mM Tris-HCl, pH 7.5, 140 mM NaCl, 1% Triton X-100, and 5 mM EDTA for 2–3 min on ice. Then, the cells were incubated in high salt buffer (as before but with 1.5 M KCl) for 20 min. After brief homogenization and centrifugation, the pellet obtained was washed several times with PBS (cytoskeletal fraction).

### Gel electrophoresis, IPs, and immunoblotting

SDS-PAGE was essentially as previously described (Achtstaetter et al., 1986; Schäfer et al., 1994; Rickelt et al., 2009). For IP, liver tissue pieces or loose pellets of cultured cells were taken up in Triton X-100–containing IP buffer (Triton-IP buffer: 20 mM Tris-HCl, pH 7.5, 150 mM NaCl, 5 mM EDTA or 0.5 mM $CaCl_2$, 1% Triton X-100, and 1 mM DTT plus protease inhibitors), in radioimmunoprecipitation assay (RIPA) IP buffer (20 mM Hepes, pH 7.4, 150 mM NaCl, 5 mM EDTA or 0.5 mM $CaCl_2$, 1% Triton X-100, 0.5% sodium deoxycholate, 0.1% SDS, 1 mM DTT, and protease inhibitors), or in Empigen-containing IP buffer (20 mM Tris-HCl, pH 7.5, 150 mM NaCl, 5 mM EDTA or 0.5 mM $CaCl_2$, 0.1 or 0.5% Empigen, 1 mM DTT, and protease inhibitors) and centrifuged at 16,100 *g* in a laboratory centrifuge (5414; Eppendorf) for 15 min at 4°C. The supernatant obtained was then precleared with protein G– or A–coupled magnetic beads (Dynal Dynabeads; Invitrogen) for several hours. In parallel, protein A– and/or protein G–coated magnetic beads were reacted with the specific antibodies or with unrelated antibodies (mouse myeloma IgG1; Invitrogen) in 50 mM Tris-HCl, pH 7.5, at 4°C for several hours. The precleared supernatant was then reacted with the antibody-coupled beads overnight in 4°C and washed intensely. The pellets obtained were solubilized in 20–40 µl SDS sample buffer, and the immunoprecipitates were compared by SDS-PAGE with the proteins contained in pellets and the supernatants of the preclearing steps before and after IP.

### Chemical cross-linking

Chemical cross-linking was performed using the $Cu^{2+}$-phenanthroline reaction to obtain short distance (2.05 Å) cysteine-bridged polypeptide molecules (compare, e.g., Soellner et al., 1985; Kapprell et al., 1987) or for longer cross-bridges with 1–5 mM amine-reactive reagent $BS^3$ (Perbio Science) in PBS, a noncleavable, membrane-impermeable, water-soluble lysine–lysine long distance (>11 Å) cross-linking agent (Sinz, 2003; Leitner et al., 2010). After the reaction, the cells were washed with PBS, and pellets and lysate supernatants were analyzed directly or submitted to IP as described in the preceding paragraph.

### siRNA transfections, incubations, and evaluations

The specific siRNA for human E-cadherin (cdh1; L-003877-00) and N-cadherin (cdh2; L-011605-00) as well as control siRNAs (nontargeting control siRNA; ON-TARGETplus SMARTpool; see Pieperhoff et al., 2008) and lamin A/C siRNA (specific for human, mouse, and rat lamin A/C; Pieperhoff et al., 2008) were purchased from Thermo Fisher Scientific. All siRNA transfections were essentially performed according to the manufacturer's protocols using lipid-based transfection reagents (DharmaFECT no. 1 or 4; Thermo Fisher Scientific; for methods of evaluation see Pieperhoff et al., 2008).

### Online supplemental material

Fig. S1 shows the extensive colocalization of E- and N-cadherin in normal murine (rat) and bovine liver tissue. Fig. S2 shows the near-complete colocalization of E- and N-cadherin in human pancreatic duct epithelium. Fig. S3 presents immunoblot detection of E- and N-cadherin upon siRNA-mediated interference in cultured hepatocellular carcinoma cells of line PLC. Table S1 lists the antibodies used in this study for protein detection and characterization. Online supplemental material is available at http://www.jcb.org/cgi/content/full/jcb.201106023/DC1.

We thank Michaela Hergt, Edeltraut Noffz, and Heiderose Schumacher for cell cultures and Elisabeth Specht-Delius for immunohistochemical work as well as Drs. Judit Boda-Heggemann, Frank-Ulrich Pape, and Oscar Cahyadi for their contributions in some of the initial experiments. Thanks go also to Dr. Thomas Longerich and to Dr. Esther Herpel for providing cryopreserved human tissue samples.

This work was supported by grants of the Ministry of Science, Research and the Arts of Baden-Wuerttemberg (grant 23-7532.22-23-12/1 to B.K. Straub and W.W. Franke), the Federal Ministry for Research and Technology (Standardization for Regenerative Therapy–Mesenchymal Stem Cells grant 01GN0942 to W.W. Franke), and a grant of the Deutsche Krebshilfe (grant 10-2049 to W.W. Franke). B.K. Straub has been supported by a stipend of the Olympia-Morata program of the Medical Faculty of Heidelberg University.

Submitted: 3 June 2011
Accepted: 25 October 2011

## References

Achtstaetter, T., M. Hatzfeld, R.A. Quinlan, D.C. Parmelee, and W.W. Franke. 1986. Separation of cytokeratin polypeptides by gel electrophoretic and chromatographic techniques and their identification by immunoblotting. *Methods Enzymol.* 134:355–371. http://dx.doi.org/10.1016/0076-6879(86)34102-8

Adams, C.L., Y.T. Chen, S.J. Smith, and W.J. Nelson. 1998. Mechanisms of epithelial cell–cell adhesion and cell compaction revealed by high-resolution tracking of E-cadherin–green fluorescent protein. *J. Cell Biol.* 142:1105–1119. http://dx.doi.org/10.1083/jcb.142.4.1105

Akhtar, N., and N.A. Hotchin. 2001. RAC1 regulates adherens junctions through endocytosis of E-cadherin. *Mol. Biol. Cell*. 12:847–862.

Alexandrova, K., C. Griesel, M. Barthold, H.G. Heuft, M. Ott, M. Winkler, H. Schrem, M.P. Manns, T. Bredehorn, M. Net, et al. 2005. Large-scale isolation of human hepatocytes for therapeutic application. *Cell Transplant.* 14:845–853. http://dx.doi.org/10.3727/000000005783982530

Behrens, J., M.M. Mareel, F.M. Van Roy, and W. Birchmeier. 1989. Dissecting tumor cell invasion: epithelial cells acquire invasive properties after the loss of uvomorulin-mediated cell–cell adhesion. *J. Cell Biol.* 108:2435–2447. http://dx.doi.org/10.1083/jcb.108.6.2435

Behrens, J., L. Vakaet, R. Friis, E. Winterhager, F. Van Roy, M.M. Mareel, and W. Birchmeier. 1993. Loss of epithelial differentiation and gain of invasiveness correlates with tyrosine phosphorylation of the E-cadherin/β-catenin complex in cells transformed with a temperature-sensitive v-SRC gene. *J. Cell Biol.* 120:757–766. http://dx.doi.org/10.1083/jcb.120.3.757

Berx, G., and F. van Roy. 2009. Involvement of members of the cadherin superfamily in cancer. *Cold Spring Harb. Perspect. Biol.* 1:a003129. http://dx.doi.org/10.1101/cshperspect.a003129

Birchmeier, W., K.M. Weidner, and J. Behrens. 1993. Molecular mechanisms leading to loss of differentiation and gain of invasiveness in epithelial cells. *J. Cell Sci. Suppl.* 17:159–164.

Blaschuk, O.W., and E. Devemy. 2009. Cadherins as novel targets for anticancer therapy. *Eur. J. Pharmacol.* 625:195–198. http://dx.doi.org/10.1016/j.ejphar.2009.05.033

Borenfreund, E., E. Schmid, A. Bendich, and W.W. Franke. 1980. Constitutive aggregates of intermediate-sized filaments of the vimentin and cytokeratin type in cultured hepatoma cells and their dispersal by butyrate. *Exp. Cell Res.* 127:215–235. http://dx.doi.org/10.1016/0014-4827(80)90428-0

Capaldo, C.T., and I.G. Macara. 2007. Depletion of E-cadherin disrupts establishment but not maintenance of cell junctions in Madin-Darby canine kidney epithelial cells. *Mol. Biol. Cell*. 18:189–200. http://dx.doi.org/10.1091/mbc.E06-05-0471

Cavallaro, U., and G. Christofori. 2004. Cell adhesion and signalling by cadherins and Ig-CAMs in cancer. *Nat. Rev. Cancer*. 4:118–132. http://dx.doi.org/10.1038/nrc1276

Chitaev, N.A., and S.M. Troyanovsky. 1998. Adhesive but not lateral E-cadherin complexes require calcium and catenins for their formation. *J. Cell Biol.* 142:837–846. http://dx.doi.org/10.1083/jcb.142.3.837

Cho, S.B., K.H. Lee, J.H. Lee, S.Y. Park, W.S. Lee, C.H. Park, H.S. Kim, S.K. Choi, and J.S. Rew. 2008. Expression of E- and N-cadherin and clinicopathology in hepatocellular carcinoma. *Pathol. Int.* 58:635–642. http://dx.doi.org/10.1111/j.1440-1827.2008.02282.x

de Beco, S., C. Gueudry, F. Amblard, and S. Coscoy. 2009. Endocytosis is required for E-cadherin redistribution at mature adherens junctions. *Proc. Natl. Acad. Sci. USA*. 106:7010–7015. http://dx.doi.org/10.1073/pnas.0811253106

Demlehner, M.P., S. Schäfer, C. Grund, and W.W. Franke. 1995. Continual assembly of half-desmosomal structures in the absence of cell contacts and their frustrated endocytosis: a coordinated Sisyphus cycle. *J. Cell Biol.* 131:745–760. http://dx.doi.org/10.1083/jcb.131.3.745

De Smet, K., S. Beken, T. Vanhaecke, M. Pauwels, A. Vercruysse, and V. Rogiers. 1998. Isolation of rat hepatocytes. *Methods Mol. Biol.* 107:295–301.

Doi, Y., S. Tamura, T. Nammo, K. Fukui, S. Kiso, and A. Nagafuchi. 2007. Development of complementary expression patterns of E- and N-cadherin in the mouse liver. *Hepatol. Res.* 37:230–237. http://dx.doi.org/10.1111/j.1872-034X.2007.00028.x

Duden, R., and W.W. Franke. 1988. Organization of desmosomal plaque proteins in cells growing at low calcium concentrations. *J. Cell Biol.* 107:1049–1063. http://dx.doi.org/10.1083/jcb.107.3.1049

Duguay, D., R.A. Foty, and M.S. Steinberg. 2003. Cadherin-mediated cell adhesion and tissue segregation: qualitative and quantitative determinants. *Dev. Biol.* 253:309–323. http://dx.doi.org/10.1016/S0012-1606(02)00016-7

Foty, R.A., and M.S. Steinberg. 2005. The differential adhesion hypothesis: a direct evaluation. *Dev. Biol.* 278:255–263. http://dx.doi.org/10.1016/j.ydbio.2004.11.012

Franke, W.W. 2009. Discovering the molecular components of intercellular junctions—a historical view. *Cold Spring Harb. Perspect. Biol.* 1:a003061. http://dx.doi.org/10.1101/cshperspect.a003061

Franke, W.W., and S. Rickelt. 2011. Mesenchymal-epithelial transitions: Spontaneous and cumulative syntheses of epithelial marker molecules and their assemblies to novel cell junctions connecting human hematopoietic tumor cells to carcinomatoid tissue structures. *Int. J. Cancer*. 129:2588–2599. http://dx.doi.org/10.1002/ijc.26227

Franke, W.W., E. Schmid, J. Kartenbeck, D. Mayer, H.J. Hacker, P. Bannasch, M. Osborn, K. Weber, H. Denk, J.-C. Wanson, and P. Drochmans. 1979. Characterization of the intermediate-sized filaments in liver cells by immunofluorescence and electron microscopy. *Biol. Cell.* 34:99–110.

Franke, W.W., H. Denk, R. Kalt, and E. Schmid. 1981a. Biochemical and immunological identification of cytokeratin proteins present in hepatocytes of mammalian liver tissue. *Exp. Cell Res.* 131:299–318. http://dx.doi.org/10.1016/0014-4827(81)90234-2

Franke, W.W., D. Mayer, E. Schmid, H. Denk, and E. Borenfreund. 1981b. Differences of expression of cytoskeletal proteins in cultured rat hepatocytes and hepatoma cells. *Exp. Cell Res.* 134:345–365. http://dx.doi.org/10.1016/0014-4827(81)90435-3

Frixen, U.H., J. Behrens, M. Sachs, G. Eberle, B. Voss, A. Warda, D. Löchner, and W. Birchmeier. 1991. E-cadherin–mediated cell–cell adhesion prevents invasiveness of human carcinoma cells. *J. Cell Biol.* 113:173–185. http://dx.doi.org/10.1083/jcb.113.1.173

Govindarajan, R., S. Chakraborty, K.E. Johnson, M.M. Falk, M.J. Wheelock, K.R. Johnson, and P.P. Mehta. 2010. Assembly of connexin43 into gap junctions is regulated differentially by E-cadherin and N-cadherin in rat liver epithelial cells. *Mol. Biol. Cell*. 21:4089–4107. http://dx.doi.org/10.1091/mbc.E10-05-0403

Gumbiner, B.M. 2005. Regulation of cadherin-mediated adhesion in morphogenesis. *Nat. Rev. Mol. Cell Biol.* 6:622–634. http://dx.doi.org/10.1038/nrm1699

Halbleib, J.M., and W.J. Nelson. 2006. Cadherins in development: cell adhesion, sorting, and tissue morphogenesis. *Genes Dev.* 20:3199–3214. http://dx.doi.org/10.1101/gad.1486806

Hatta, K., and M. Takeichi. 1986. Expression of N-cadherin adhesion molecules associated with early morphogenetic events in chick development. *Nature*. 320:447–449. http://dx.doi.org/10.1038/320447a0

Hazan, R.B., G.R. Phillips, R.F. Qiao, L. Norton, and S.A. Aaronson. 2000. Exogenous expression of N-cadherin in breast cancer cells induces cell migration, invasion, and metastasis. *J. Cell Biol.* 148:779–790. http://dx.doi.org/10.1083/jcb.148.4.779

Higashi, N., N. Kojima, M. Miura, K. Imai, M. Sato, and H. Senoo. 2004. Cell-cell junctions between mammalian (human and rat) hepatic stellate cells. *Cell Tissue Res.* 317:35–43. http://dx.doi.org/10.1007/s00441-004-0891-9

Hong, S., R.B. Troyanovsky, and S.M. Troyanovsky. 2010. Spontaneous assembly and active disassembly balance adherens junction homeostasis. *Proc. Natl. Acad. Sci. USA*. 107:3528–3533. http://dx.doi.org/10.1073/pnas.0911027107

Ihara, A., H. Koizumi, R. Hashizume, and T. Uchikoshi. 1996. Expression of epithelial cadherin and alpha- and beta-catenins in nontumoral livers and hepatocellular carcinomas. *Hepatology*. 23:1441–1447.

Inayoshi, J., T. Ichida, S. Sugitani, Y. Tsuboi, T. Genda, N. Honma, and H. Asakura. 2003. Gross appearance of hepatocellular carcinoma reflects E-cadherin expression and risk of early recurrence after surgical treatment. *J. Gastroenterol. Hepatol.* 18:673–677. http://dx.doi.org/10.1046/j.1440-1746.2003.03021.x

Johnson, K.R., J.E. Lewis, D. Li, J. Wahl, A.P. Soler, K.A. Knudsen, and M.J. Wheelock. 1993. P- and E-cadherin are in separate complexes in cells expressing both cadherins. *Exp. Cell Res.* 207:252–260. http://dx.doi.org/10.1006/excr.1993.1191

Kalluri, R., and R.A. Weinberg. 2009. The basics of epithelial-mesenchymal transition. *J. Clin. Invest.* 119:1420–1428. http://dx.doi.org/10.1172/JCI39104

Kan, N.G., M.P. Stemmler, D. Junghans, B. Kanzler, W.N. de Vries, M. Dominis, and R. Kemler. 2007. Gene replacement reveals a specific role for E-cadherin in the formation of a functional trophectoderm. *Development*. 134:31–41. http://dx.doi.org/10.1242/dev.02722

Kapprell, H.P., P. Cowin, and W.W. Franke. 1987. Biochemical characterization of the soluble form of the junctional plaque protein, plakoglobin, from different cell types. *Eur. J. Biochem.* 166:505–517. http://dx.doi.org/10.1111/j.1432-1033.1987.tb13543.x

Kartenbeck, J., E. Schmid, W.W. Franke, and B. Geiger. 1982. Different modes of internalization of proteins associated with adhaerens junctions and desmosomes: experimental separation of lateral contacts induces endocytosis of desmosomal plaque material. *EMBO J.* 1:725–732.

Kartenbeck, J., M. Schmelz, W.W. Franke, and B. Geiger. 1991. Endocytosis of junctional cadherins in bovine kidney epithelial (MDBK) cells cultured in low Ca2+ ion medium. *J. Cell Biol.* 113:881–892. http://dx.doi.org/10.1083/jcb.113.4.881

Katsamba, P., K. Carroll, G. Ahlsen, F. Bahna, J. Vendome, S. Posy, M. Rajebhosale, S. Price, T.M. Jessell, A. Ben-Shaul, et al. 2009. Linking molecular affinity and cellular specificity in cadherin-mediated adhesion. *Proc. Natl. Acad. Sci. USA*. 106:11594–11599. http://dx.doi.org/10.1073/pnas.0905349106

Kern, M.A., D. Schubert, D. Sahi, M.M. Schöneweiss, I. Moll, A.M. Haugg, H.P. Dienes, K. Breuhahn, and P. Schirmacher. 2002. Proapoptotic and antiproliferative potential of selective cyclooxygenase-2 inhibitors in human liver tumor cells. *Hepatology*. 36:885–894.

Kim, J.B., S. Islam, Y.J. Kim, R.S. Prudoff, K.M. Sass, M.J. Wheelock, and K.R. Johnson. 2000. N-Cadherin extracellular repeat 4 mediates epithelial to mesenchymal transition and increased motility. *J. Cell Biol.* 151:1193–1206. http://dx.doi.org/10.1083/jcb.151.6.1193

Kozyraki, R., J.Y. Scoazec, J.F. Flejou, A. D'Errico, P. Bedossa, B. Terris, M. Fiorentino, A.F. Bringuier, W.F. Grigioni, and G. Feldmann. 1996. Expression of cadherins and alpha-catenin in primary epithelial tumors of the liver. *Gastroenterology*. 110:1137–1149. http://dx.doi.org/10.1053/gast.1996.v110.pm8613003

Le, T.L., A.S. Yap, and J.L. Stow. 1999. Recycling of E-cadherin: a potential mechanism for regulating cadherin dynamics. *J. Cell Biol.* 146:219–232.

Leitner, A., T. Walzthoeni, A. Kahraman, F. Herzog, O. Rinner, M. Beck, and R. Aebersold. 2010. Probing native protein structures by chemical cross-linking, mass spectrometry, and bioinformatics. *Mol. Cell. Proteomics*. 9:1634–1649. http://dx.doi.org/10.1074/mcp.R000001-MCP201

Libusova, L., M.P. Stemmler, A. Hierholzer, H. Schwarz, and R. Kemler. 2010. N-cadherin can structurally substitute for E-cadherin during intestinal development but leads to polyp formation. *Development*. 137:2297–2305. http://dx.doi.org/10.1242/dev.048488

Maeda, M., K.R. Johnson, and M.J. Wheelock. 2005. Cadherin switching: essential for behavioral but not morphological changes during an epithelium-to-mesenchyme transition. *J. Cell Sci.* 118:873–887. http://dx.doi.org/10.1242/jcs.01634

Mareel, M.M., J. Behrens, W. Birchmeier, G.K. De Bruyne, K. Vleminckx, A. Hoogewijs, W.C. Fiers, and F.M. Van Roy. 1991. Down-regulation of E-cadherin expression in Madin Darby canine kidney (MDCK) cells inside tumors of nude mice. *Int. J. Cancer*. 47:922–928. http://dx.doi.org/10.1002/ijc.2910470623

Nieman, M.T., R.S. Prudoff, K.R. Johnson, and M.J. Wheelock. 1999. N-cadherin promotes motility in human breast cancer cells regardless of their E-cadherin expression. *J. Cell Biol.* 147:631–644. http://dx.doi.org/10.1083/jcb.147.3.631

Niessen, C.M., and B.M. Gumbiner. 2002. Cadherin-mediated cell sorting not determined by binding or adhesion specificity. *J. Cell Biol.* 156:389–399. http://dx.doi.org/10.1083/jcb.200108040

Nuruki, K., H. Toyoyama, S. Ueno, M. Hamanoue, G. Tanabe, T. Aikou, and M. Ozawa. 1998. E-cadherin but not N-cadherin expression is correlated with the intracellular distribution of catenins in human hepatocellular carcinomas. *Oncol. Rep.* 5:1109–1114.

Ochiai, A., Y. Kanai, and S. Hirohashi. 1999. Multiple mechanisms for inactivation of E-cadherin cell adhesion system in cancer. *In* Epithelial Morphogenesis in Development and Disease. W. Birchmeier and C. Birchmeier, editors. Harwood Academic Publishers, Amsterdam. 427–444.

Ozawa, M. 2002. Lateral dimerization of the E-cadherin extracellular domain is necessary but not sufficient for adhesive activity. *J. Biol. Chem.* 277: 19600–19608. http://dx.doi.org/10.1074/jbc.M202029200

Perez, T.D., and W.J. Nelson. 2004. Cadherin adhesion: mechanisms and molecular interactions. *Handb Exp Pharmacol*. 165:3–21. http://dx.doi.org/10.1007/978-3-540-68170-0_1

Peters, S.J., T. Vanhaecke, P. Papeleu, V. Rogiers, H.P. Haagsman, and K. van Norren. 2010. Co-culture of primary rat hepatocytes with rat liver epithelial cells enhances interleukin-6-induced acute-phase protein response. *Cell Tissue Res.* 340:451–457. http://dx.doi.org/10.1007/s00441-010-0955-y

Pieperhoff, S., H. Schumacher, and W.W. Franke. 2008. The area composita of adhering junctions connecting heart muscle cells of vertebrates. V. The importance of plakophilin-2 demonstrated by small interference RNA-mediated knockdown in cultured rat cardiomyocytes. *Eur. J. Cell Biol.* 87:399–411. http://dx.doi.org/10.1016/j.ejcb.2007.12.002

Rickelt, S., S. Winter-Simanowski, E. Noffz, C. Kuhn, and W.W. Franke. 2009. Upregulation of plakophilin-2 and its acquisition to adherens junctions identifies a novel molecular ensemble of cell-cell-attachment characteristic for transformed mesenchymal cells. *Int. J. Cancer*. 125:2036–2048. http://dx.doi.org/10.1002/ijc.24552

Schäfer, S., P.J. Koch, and W.W. Franke. 1994. Identification of the ubiquitous human desmoglein, Dsg2, and the expression catalogue of the desmoglein subfamily of desmosomal cadherins. *Exp. Cell Res.* 211:391–399. http://dx.doi.org/10.1006/excr.1994.1103

Seglen, P.O. 1979. Hepatocyte suspensions and cultures as tools in experimental carcinogenesis. *J. Toxicol. Environ. Health*. 5:551–560. http://dx.doi.org/10.1080/15287397909529766

Shan, W.S., H. Tanaka, G.R. Phillips, K. Arndt, M. Yoshida, D.R. Colman, and L. Shapiro. 2000. Functional cis-heterodimers of N- and R-cadherins. *J. Cell Biol.* 148:579–590. http://dx.doi.org/10.1083/jcb.148.3.579

Shapiro, L., and W.I. Weis. 2009. Structure and biochemistry of cadherins and catenins. *Cold Spring Harb. Perspect. Biol.* 1:a003053. http://dx.doi.org/10.1101/cshperspect.a003053

Sinz, A. 2003. Chemical cross-linking and mass spectrometry for mapping three-dimensional structures of proteins and protein complexes. *J. Mass Spectrom.* 38:1225–1237. http://dx.doi.org/10.1002/jms.559

Soellner, P., R.A. Quinlan, and W.W. Franke. 1985. Identification of a distinct soluble subunit of an intermediate filament protein: tetrameric vimentin from living cells. *Proc. Natl. Acad. Sci. USA*. 82:7929–7933. http://dx.doi.org/10.1073/pnas.82.23.7929

Straub, B.K., J. Boda, C. Kuhn, M. Schnoelzer, U. Korf, T. Kempf, H. Spring, M. Hatzfeld, and W.W. Franke. 2003. A novel cell-cell junction system: the cortex adhaerens mosaic of lens fiber cells. *J. Cell Sci.* 116:4985–4995. http://dx.doi.org/10.1242/jcs.00815

Straub, B.K., P. Stoeffel, H. Heid, R. Zimbelmann, and P. Schirmacher. 2008. Differential pattern of lipid droplet-associated proteins and de novo perilipin expression in hepatocyte steatogenesis. *Hepatology*. 47:1936–1946. http://dx.doi.org/10.1002/hep.22268

Takeda, H. 2004. cis-Dimer formation of E-cadherin is independent of cell-cell adhesion assembly in vivo. *Biochem. Biophys. Res. Commun.* 316:822–826. http://dx.doi.org/10.1016/j.bbrc.2004.02.123

Takeda, H., Y. Shimoyama, A. Nagafuchi, and S. Hirohashi. 1999. E-cadherin functions as a cis-dimer at the cell-cell adhesive interface in vivo. *Nat. Struct. Biol.* 6:310–312. http://dx.doi.org/10.1038/7542

Takeichi, M. 1988. The cadherins: cell-cell adhesion molecules controlling animal morphogenesis. *Development*. 102:639–655.

Takeichi, M. 1993. Cadherins in cancer: implications for invasion and metastasis. *Curr. Opin. Cell Biol.* 5:806–811. http://dx.doi.org/10.1016/0955-0674(93)90029-P

Takeichi, M. 1995. Morphogenetic roles of classic cadherins. *Curr. Opin. Cell Biol.* 7:619–627. http://dx.doi.org/10.1016/0955-0674(95)80102-2

Théard, D., M. Steiner, D. Kalicharan, D. Hoekstra, and S.C. van Ijzendoorn. 2007. Cell polarity development and protein trafficking in hepatocytes lacking E-cadherin/beta-catenin-based adherens junctions. *Mol. Biol. Cell*. 18:2313–2321. http://dx.doi.org/10.1091/mbc.E06-11-1040

Théard, D., M.A. Raspe, D. Kalicharan, D. Hoekstra, and S.C. van IJzendoorn. 2008. Formation of E-cadherin/beta-catenin-based adherens junctions in hepatocytes requires serine-10 in p27(Kip1). *Mol. Biol. Cell*. 19:1605–1613. http://dx.doi.org/10.1091/mbc.E07-07-0661

Thiery, J.P., H. Acloque, R.Y. Huang, and M.A. Nieto. 2009. Epithelial-mesenchymal transitions in development and disease. *Cell*. 139:871–890. http://dx.doi.org/10.1016/j.cell.2009.11.007

Troyanovsky, S. 2005. Cadherin dimers in cell-cell adhesion. *Eur. J. Cell Biol.* 84:225–233. http://dx.doi.org/10.1016/j.ejcb.2004.12.009

Tsuchiya, B., Y. Sato, T. Kameya, I. Okayasu, and K. Mukai. 2006. Differential expression of N-cadherin and E-cadherin in normal human tissues. *Arch. Histol. Cytol.* 69:135–145. http://dx.doi.org/10.1679/aohc.69.135

Vleminckx, K., L. Vakaet Jr., M. Mareel, W. Fiers, and F. van Roy. 1991. Genetic manipulation of E-cadherin expression by epithelial tumor cells reveals an invasion suppressor role. *Cell*. 66:107–119. http://dx.doi.org/10.1016/0092-8674(91)90143-M

Volk, T., O. Cohen, and B. Geiger. 1987. Formation of heterotypic adherens-type junctions between L-CAM-containing liver cells and A-CAM-containing lens cells. *Cell*. 50:987–994. http://dx.doi.org/10.1016/0092-8674(87)90525-3

Wei, Y., J.T. Van Nhieu, S. Prigent, P. Srivatanakul, P. Tiollais, and M.A. Buendia. 2002. Altered expression of E-cadherin in hepatocellular carcinoma: correlations with genetic alterations, beta-catenin expression, and clinical features. *Hepatology*. 36:692–701. http://dx.doi.org/10.1053/jhep.2002.35342

Wheelock, M.J., and K.R. Johnson. 2003. Cadherins as modulators of cellular phenotype. *Annu. Rev. Cell Dev. Biol.* 19:207–235. http://dx.doi.org/10.1146/annurev.cellbio.19.011102.111135

Wheelock, M.J., Y. Shintani, M. Maeda, Y. Fukumoto, and K.R. Johnson. 2008. Cadherin switching. *J. Cell Sci.* 121:727–735. http://dx.doi.org/10.1242/jcs.000455

Yamazaki, Y., K. Okawa, T. Yano, S. Tsukita, and S. Tsukita. 2008. Optimized proteomic analysis on gels of cell-cell adhering junctional membrane proteins. *Biochemistry*. 47:5378–5386. http://dx.doi.org/10.1021/bi8002567

Yap, A.S., C.M. Niessen, and B.M. Gumbiner. 1998. The juxtamembrane region of the cadherin cytoplasmic tail supports lateral clustering, adhesive strengthening, and interaction with $p120^{ctn}$. *J. Cell Biol.* 141:779–789. http://dx.doi.org/10.1083/jcb.141.3.779

Yilmaz, M., and G. Christofori. 2009. EMT, the cytoskeleton, and cancer cell invasion. *Cancer Metastasis Rev.* 28:15–33. http://dx.doi.org/10.1007/s10555-008-9169-0

Zhang, Y., S. Sivasankar, W.J. Nelson, and S. Chu. 2009. Resolving cadherin interactions and binding cooperativity at the single-molecule level. *Proc. Natl. Acad. Sci. USA*. 106:109–114. http://dx.doi.org/10.1073/pnas.0811350106